

General Disclaimer

One or more of the Following Statements may affect this Document

- This document has been reproduced from the best copy furnished by the organizational source. It is being released in the interest of making available as much information as possible.
- This document may contain data, which exceeds the sheet parameters. It was furnished in this condition by the organizational source and is the best copy available.
- This document may contain tone-on-tone or color graphs, charts and/or pictures, which have been reproduced in black and white.
- This document is paginated as submitted by the original source.
- Portions of this document are not fully legible due to the historical nature of some of the material. However, it is the best reproduction available from the original submission.

(NASA-CR-163612) THE DYNAMICS AND CONTROL
OF LARGE FLEXIBLE SPACE STRUCTURES. VOLUME
3, PART B: THE MODELLING, DYNAMICS, AND
STABILITY OF LARGE EARTH POINTING ORBITING
STRUCTURES Final Report (Howard Univ.)

N80-33449

Unclas
G3/14 28947



HOWARD UNIVERSITY
SCHOOL OF ENGINEERING
DEPARTMENT OF MECHANICAL ENGINEERING
WASHINGTON, D.C. 20059

FINAL REPORT

NASA GRANT: NSG-1414, Suppl. 2

THE DYNAMICS AND CONTROL OF LARGE
FLEXIBLE SPACE STRUCTURES - III

val.

PART B: THE MODELLING, DYNAMICS, AND STABILITY
OF LARGE EARTH POINTING ORBITING STRUCTURES

by

Peter M. Bainum
Professor of Aerospace Engineering
Principal Investigator

and

V.K. Kumar
Graduate Research Assistant
September 1980

ABSTRACT

The dynamics and stability of large orbiting flexible beams, and platforms and dish type structures oriented along the local horizontal are treated both analytically and numerically. It is assumed that such structures could be gravitationally stabilized by attaching a rigid lightweight dumbbell at the center of mass by a spring loaded hinge which also could provide viscous damping. For the beam it is seen that the small amplitude inplane pitch motion, dumbbell librational motion, and the anti-symmetric elastic modes are all coupled. The three dimensional equations of motion for a circular flat plate and shallow spherical shell in orbit with a two-degree-of freedom gimbaled dumbbell are also developed and show that only those elastic modes described by a single nodal diameter line are influenced by the dumbbell motion. Further, in the case of shallow spherical shells the pitch and the axi-symmetric modes are seen to be weakly coupled in the linear range. With the shell's symmetry axis following the local vertical, the structure undergoes a static deformation under the influence of gravity and inertia. Stability criteria are developed for all the examples and a sensitivity study of the system response characteristics to the key system parameters is carried out.

CONTENTS

ABSTRACT

LIST OF FIGURES

NOMENCLATURE

CHAPTER 1 - INTRODUCTION

CHAPTER 2 - EQUATIONS OF MOTION OF AN ARBITRARY FLEXIBLE
BODY IN ORBIT

CHAPTER 3 - ON THE DYNAMICS OF LARGE ORBITING FLEXIBLE
BEAMS AND PLATFORMS ORIENTED ALONG THE
LOCAL HORIZONTAL

CHAPTER 4 - ON THE MOTION OF A FLEXIBLE SHALLOW SPHERICAL
SHELL IN ORBIT

CONCLUSIONS

RECOMMENDATIONS

APPENDIX A

APPENDIX B

APPENDIX C

LIST OF FIGURES

Chapter 3

- Fig. 1 - Dumbbell Stabilized Flexible Beam with Nominal Orientation Along Local Horizontal
- Fig. 2 - Variations in the Root Loci of the Least Damped Mode with Beam Stiffness and Dumbbell Restoring Characteristics
- Fig. 3 - Time Response of Dumbbell Stabilized Flexible Beam in Orbit
- Fig. 4 - Flexible Circular Plate Nominally in the Local Horizontal Plane with the Stabilizing Dumbbell
- Fig. 5 - Root Locus of Least Damped Mode - Rigid Circular Plate with Dumbbell
- Fig. 6 - Root Locus of Least Damped Mode - Circular Plate with Dumbbell

Chapter 4

- Fig. 4.1a - Shallow Spherical Shell
- Fig. 4.1b - Shallow Spherical Shell with Dumbbell
- Fig. 4.2 - Root Locus of Least Damped Mode-Rigid Shallow Spherical Shell
- Fig. 4.3 - Root Locus of Lowest Frequency Mode - Shallow Spherical Shell with Dumbbell (Nodal Diameter Along Pitch Axis)
- Fig. 4.4 - Root Locus of Lowest Frequency Mode - Shallow Spherical Shell with Dumbbell (Nodal Diameter Along Roll Axis)

NOMENCLATURE

- A, A_1, A_2 : system matrices
- A_n : modal amplitudes
- \bar{a}_{cm} : inertial acceleration of the center of mass
- \bar{C} : external torques with components (C_x, C_y, C_z)
- c, c_y, c_z : co-efficients of viscous damping
- $\bar{c}, \bar{c}_y, \bar{c}_z$: $c/J_y \omega_c, c_y/J_y \omega_c, c_z/J_z \omega_c$ respectively
- $C_y^{(n)}, C_z^{(n)}$: $\frac{\partial \phi_x^{(n)}}{\partial y} (0,0), \frac{\partial \phi_x^{(n)}}{\partial z} (0,0)$, respectively
- $C_y^{(mn)}, C_z^{(mn)}$: $\frac{J_y}{M \ell^2} C_y^{(m)} C_y^{(n)}, \frac{J_z}{M \ell^2} C_z^{(m)} C_z^{(n)}$
- c_1 : J_y/I_d
- c_2 : J_z/I_d
- c_3 : $J_y/m\ell^2$
- D'_n : center of mass shift term in eq. (2.3)
- $\bar{D}^{(n)}$: center of mass shift term in eq. (2.2)
- D : flexural rigidity, $Eh^3/12(1-\nu^2)$
- E_n : modal component of external forces
- $(\hat{e}_r, \hat{e}_\beta, \hat{i})$: unit vectors in local cylindrical frame
- \bar{e} : external force per unit mass
- \bar{F}_0 : gravitational force per unit mass at the center of mass of the body
- \bar{F}_d : gravity force at the dumbbell
- $\bar{G}^{(n)}$: gravity torque in eq. (2.2)

\overline{G}_R	: gravity torque in eq. (2.2), with components ($G_{R_x}, G_{R_y}, G_{R_z}$)
\overline{G}_d	: gravity torque on dumbbell, with components ($G_{x_d}, G_{y_d}, G_{z_d}$)
g_n, g_{nm}	: coupling terms in eq. (2.3)
I	: identity matrix
I_d	: moment of inertia of the dumbbell
I_1, \dots, I_7	: volume integrals defined in eqns. (4.21)-(4.26)
$I_{x_0}^{(j)}, I_{x_2}^{(j)}, I_r^{(j)}$: integrals defined in eqns. (4.30)-(5.34), superscript j represents number of nodal circles ($j = 1, 2, \dots$)
$\hat{i}, \hat{j}, \hat{k}$: unit vectors along the principal axes of the undeformed body
J_x, J_y, J_z	: principal moments of inertia of the undeformed body
k, k_y, k_z	: torsional spring constants
$\overline{k}, \overline{k}_y, \overline{k}_z$: $k/J_y \omega_c^2, k_y/J_y \omega_c^2, k_z/J_z \omega_c^2$, respectively
l	: characteristic length (length of the beam, radius of circular plate, etc.)
$2l_d$: length of the dumbbell
M	: gravity gradient matrix operator with elements M_{ij}
M_n	: modal mass of n^{th} mode
m	: mass of beam, plate or shell
m_d	: tip mass of the dumbbell
m_t	: mass of the concentrated mass placed at the end of diameter of circular plate
O	: null matrix
$\overline{Q}^{(n)}$: inertia torque, eq. (2.2)
\overline{q}	: elastic displacement vector, $(q_x, q_y, q_z)^T$

R : radius of curvature of the shell
 \bar{R} : inertia tensor, eq. (2.2)
 \bar{r} : instantaneous position vector of generic point in the body
 r_0 : position vector of generic point in the undeformed body, (ξ_x, ξ_y, ξ_z)
 \bar{r}_1 : vector from the mass center of the shell to the origin of (x_c, y_c, z_c)
 \bar{r}_2 : position vector of a generic point on undeformed shell in, (x_c, y_c, z_c)
 r_c : radial distance of the shell element from the symmetry axis of the shell
 T_1, T_2, T_3, T_4 : coordinate transformation matrices
 t : time
 α : angle between dumbbell and local vertical
 α_i : coefficients
 β : polar angle
 β_0 : phase angle
 (γ, δ) : dumbbell deflection angles
 δ_{mn} : Kronecker delta
 ε_n : A_n / ℓ
 ζ : damping ratio
 σ : rotation of the beam at the center due to elastic deformation
 σ_y, σ_z : small rotations at the origin about y and z axes due to elastic deformations
 $\lambda_{j,p}$: frequency parameter; j = no. of nodal circles; p = no. of nodal diameters
 θ, ψ, ϕ : pitch, yaw and roll angles
 X, X_1, X_2 : state vectors

- ρ : mass density
 τ : $\omega_c t$
 τ_b : body frame, (xyz)
 τ_c : coordinate frame, ($x_c y_c z_c$)
 τ_d : dumbbell frame ($x_d y_d z_d$)
 τ_o : orbit frame, ($x_o y_o z_o$)
 $\phi^{(n)}$: mode shape vector, ($\phi_x^{(n)}, \phi_y^{(n)}, \phi_z^{(n)}$)
 Φ_n, Φ_{mn} : coupling terms in eq. (2.3)
 $\bar{\omega}$: body angular velocity vector, ($\omega_x \omega_y \omega_z$) or $\omega_r \omega_\beta \omega_x$
 ω_c : orbit angular velocity
 ω_n : natural frequency of n^{th} mode
 $(\omega_x \omega_y \omega_z)$: angular velocity components of dumbbell
 $\bar{\omega}_n$: ω_n / ω_c
 $\Omega_x, \Omega_y, \Omega_z$: $(J_z - J_y) / J_x, (J_x - J_z) / J_y, (J_y - J_x) / J_z$
 $(\dot{})$: $\frac{d}{dt}$
 $()'$: $\frac{d}{d\tau}$

CHAPTER 1

INTRODUCTION

This represents the second part of the 1979-80 final report and concentrates on the modelling, dynamics, and stability of large, flexible earth pointing orbiting structures. First, a brief review of the general formulation (continuum model) for any large flexible space system in orbit, as previously developed^{*1,2} is summarized in Chapter 2.

The paper to be presented at a forthcoming conference forms the basis of Chapter 3: "On the Dynamics and Control of Large Orbiting Flexible Beams and Platforms Oriented along the Local Horizontal," XXXIst Congress of the International Astronautical Federation, Sept. 21-28, 1980, IAF-80-E-230. This section treats the uncontrolled dynamics of a large thin flexible beam in orbit with emphasis placed on the motion about the local horizontal orientation instead of the local vertical. The use of a gimbaled connected dumbbell is proposed to provide the correct composite moment of inertia ratio required for gravitational stabilization and to also offer a restoring torque (and possibly damping torque) due to the spring-gimball assembly. A further extension of this concept considers the use of a two-degree-of-freedom gimbaled dumbbell to aid in the stabilization of a large flexible plate (platform) in orbit about the nominal orientation in the local horizontal (tangent) plane

In Chapter 4 the treatment of Chapter 3 is extended to consider the dynamics and stability of a large flexible shallow shell structure in orbit. As in the previous formulation for the beam and plate, a stabilizing dumbbell with two degrees of freedom is also incorporated to offer gravitational stabilization characteristics.

In Chapter 5, general concluding comments and recommendations for future work to be initiated in the 1980-81 grant year, in accordance with a recent proposal³ to NASA are discussed.

* For references cited in this report, see list of references provided after each chapter.

References - Introduction

1. Bainum, Peter M., Kumar, V.K. and James, Paul K., "The Dynamics and Control of Large Flexible Space Structures," Final Report, NASA Grant: NSG-1414, Part B: Development of Continuum Model and Computer Simulation, Howard University, May 1978.
2. Bainum, Peter M., James, Paul K., Krishna, R. and Kumar, V.K., "The Dynamics and Control of Large Flexible Space Structures II," Final Report, NASA-Grant: NSG-1414, Suppl. 1, Part B: Model Development and Computer Simulation, Howard University, June 1979.
3. Bainum, Peter M., "Proposal for Research Grant on: The Dynamics and Control of Large Flexible Space Structures-IV," Howard University (submitted to NASA), Jan. 15, 1980.

CHAPTER 2

EQUATIONS OF MOTION OF AN ARBITRARY FLEXIBLE BODY IN ORBIT

A brief review of the basic equations describing the attitude motion of an arbitrary flexible body in orbit is presented here. Details regarding the derivation of these equations can be found in ref. 1.

In general, any arbitrary motion of a flexible body in space, about its center of mass, consists of a rigid body rotation about an instantaneous axis of rotation through the center of mass and elastic deformations. The rigid body rotation can be expressed by a sequence of three successive Euler angle rotations about the body fixed axes. Furthermore, if we assume small elastic deformations of the body, the elastic displacements can be expressed as the superposition of an infinite number of structural mode shapes weighted by the time dependent amplitude functions. Expressed symbolically, this appears as,

$$\bar{q}(\bar{r}_0, t) = \sum_{n=1}^{\infty} A_n(t) \phi(\bar{r}_0) \quad (2.1)$$

where, \bar{r}_0 = position vector of a generic point in the body in the undeformed state
 \bar{q} = elastic displacement vector at \bar{r}_0
 ϕ = vector of mode shape functions.

Thus, the basic equations which describe the general motion of an arbitrary flexible body in space about its center of mass consist of (n+3) equations: three equations describing rigid body rotational motion; and n-modal equations which describe the elastic motion of the body. These equations as developed in ref. 1 appear as follows;

Equations of rigid body rotation:

$$\bar{R} + \sum_n \bar{Q}^{(n)} + \sum_n \bar{D}^{(n)} = \bar{G}_R + \sum_n \bar{G}^{(n)} + \bar{C} \quad (2.2)$$

where, \bar{R} = inertia torques due to rigid body motion

$\sum_n \bar{Q}^{(n)}$ = inertia torques due to elastic motion

$\sum_n \bar{D}^{(n)}$ = torques due to center of mass shift effects
 (zero for unconstrained structures)

Ref. 1: Bainum, P.M., Kumar, V.K., James, P.K., "The Dynamics and Control of Large Flexible Space Structures," NASA CR-156976 Report, May 1978.

- \bar{G}_R = gravitational torques due to rigid body motion
 $\bar{G}_R^{(n)}$ = gravitational torques due to elastic motion
 \bar{C} = other external disturbance and control torques

Equations of elastic motion:

$$\ddot{A}_n + \omega_n^2 A_n + \frac{\Phi_n}{M_n} + \frac{1}{M_n} \sum \Phi_{mn} = \frac{1}{M_n} [g_n + \sum_m g_{mn} + D'_n + E_n] \quad (2.3)$$

where, A_n = modal amplitude

ω_n = n^{th} structural modal frequency

Φ_n = inertia coupling between the rigid body modes and n^{th} structural mode

Φ_{mn} = inertia coupling between the m^{th} and n^{th} structural modes

g_n = gravity coupling between the rigid body modes and n^{th} structural mode

g_{mn} = gravity coupling between the m^{th} and n^{th} structural mode

D'_n = term due to center of mass shift (zero for unconstrained structures)

E_n = modal component of external disturbance and control forces

M_n = n^{th} modal mass

The term \bar{R} in eq. (2.2) contains the terms from the classical Euler equations for rigid body rotations which are obtained by assuming the body to be rigid. In the body fixed principal axes reference frame, \bar{R} is given by,

$$\begin{aligned} \bar{R} = & \{J_x \dot{\omega}_x + (J_z - J_y) \omega_y \omega_z\} \hat{i} \\ & + \{J_y \dot{\omega}_y + (J_x - J_z) \omega_z \omega_x\} \hat{j} \\ & + \{J_z \dot{\omega}_z + (J_y - J_x) \omega_x \omega_y\} \hat{k} \end{aligned} \quad (2.4)$$

where, $(J_x, J_y, J_z) \approx$ principal moments of inertia of the body in the undeformed state

$(\omega_x, \omega_y, \omega_z) =$ components of the body angular velocity vector, $\bar{\omega}$, in the body principal axes frame

$\hat{i}, \hat{j}, \hat{k},$ = unit vectors along the body principal axes

The vector expressions for the other remaining terms in eqns. (2.2) and (2.3) are as follows:

$$\sum_n \bar{Q}^{(n)} = \int_v [\bar{r}_0 \times \ddot{\bar{q}} + 2\bar{r}_0 \times (\bar{\omega} \times \dot{\bar{q}}) + \bar{r}_0 \times (\dot{\bar{\omega}} \times \bar{q}) + \bar{q} \times (\dot{\bar{\omega}} \times \bar{r}_0) - (\bar{r}_0 \cdot \bar{\omega})(\bar{\omega} \times \bar{q}) - (\bar{q} \cdot \bar{\omega})(\bar{\omega} \times \bar{r}_0)] dm \quad (2.5)$$

$$\sum_n \bar{D} = \int_v \bar{q} dm \times (\bar{a}_{cm} - \bar{f}_0) + \sum_n \omega_n^2 A_n \int_{vol} \bar{r}_0 \times \phi dm \quad (2.6)$$

$$\bar{G}_R = \int_v \bar{r}_0 \times M \bar{r}_0 dm \quad (2.7)$$

$$\sum_n \bar{G}^{(n)} = \int_v [\bar{r}_0 \times M \bar{q} + \bar{q} \times M \bar{r}_0] dm \quad (2.8)$$

$$\bar{C} = \int_v \bar{r} \times \bar{e} dm \quad (2.9)$$

$$\mathcal{Q}_n = \int_v \phi^{(n)} \cdot \dot{\bar{\omega}} \times \bar{r}_0 + \phi^{(n)} \cdot \bar{\omega} \times (\bar{\omega} \times \bar{r}_0) dm \quad (2.10)$$

$$\sum_m \mathcal{Q}_{mn} = \int_v [2\phi^{(n)} \cdot \dot{\bar{\omega}} \times \bar{q} + \phi^{(n)} \cdot \dot{\bar{\omega}} \times \bar{q} + \phi^{(n)} \cdot \bar{\omega} \times (\bar{\omega} \times \bar{q})] dm \quad (2.11)$$

$$\mathcal{G}_n = \int_v \phi^{(n)} \cdot M \bar{r}_0 dm \quad (2.12)$$

$$\sum_m \mathcal{G}_{mn} = \int_v \phi^{(n)} \cdot M \bar{q} dm \quad (2.13)$$

$$D'_n = \int_v \phi dm \cdot (\bar{a}_{cm} - \bar{f}_0) \quad (2.14)$$

- where, \bar{a}_{cm} = inertial acceleration of the center of mass of the body
- \bar{f}_0 = gravitational force per unit mass at the center of mass of the body
- \bar{r} = instantaneous position vector of a generic mass point in the body
- \bar{e} = external disturbance and control forces per unit mass of the body
- M = a matrix operator dependent on the Euler angles

The mode shape vectors, $\phi^{(n)}$ ($n = 1, 2, \dots$) are orthogonal to each other, i.e.

$$\int_V \phi^{(m)} \cdot \phi^{(n)} dm = M_n \delta_{mn} \quad (2.15)$$

In addition, for unconstrained structures in space, rigid body translation and rotational modes should be orthogonal to $\phi^{(n)}$ ($n = 1, 2, \dots$) i.e.,

$$\int_V \phi^{(n)} dm = 0 \quad (2.16)$$

$$\int_V \bar{r}_0 \times \phi^{(n)} dm = 0 \quad (2.17)$$

Several specific applications of flexible spacecraft in orbit considered in the following chapters utilize the equations presented in this chapter as the basis of the formulation of their models.

Chapter 3

ON THE DYNAMICS OF LARGE ORBITING FLEXIBLE BEAMS AND PLATFORMS ORIENTED ALONG THE LOCAL HORIZONTAL

ABSTRACT

The dynamics and stability of large orbiting flexible beams and platforms oriented along the local horizontal are treated both analytically and numerically. It is assumed that such structures could be gravitationally stabilized by attaching a rigid lightweight dumbbell at the center of mass by a spring loaded hinge which also could provide viscous damping. For the beam it is seen that the small amplitude inplane pitch motion, dumbbell librational motion, and the anti-symmetric elastic modes are all coupled. The three dimensional equations of motion for a circular flat plate in orbit with a two-degree-of-freedom gimballed dumbbell are also developed and show that only those elastic modes described by a single nodal diameter line are influenced by the dumbbell motion. Stability criteria are developed for both examples and a parametric study of the least damped mode characteristics together with numerically simulated transient responses are carried out.

KEYWORDS

Flexible spacecraft dynamics; stability; stabilizing gimballed dumbbell booms; large space structures.

INTRODUCTION

Proposed future applications of large space structures include: space based power generation and transmission (to earth); communications; earth resource observation missions; and electronic mail systems.

Through the use of such systems, one can see an example of the applications of space developments to solve some of the problems of mankind such as in education, economy, and energy. The applications described here all require that the largest surface (length) of the system be nominally oriented along the orbital tangent or normal to the local vertical. To gain insight into the types of problems involved with inherently complex space structures, two simple examples of large flexible space systems are addressed in this paper. It should be recognized that beams and plate elements would be two of the most fundamental structural elements in any large space structural system.

Previously the equations of motion of a general arbitrary flexible spacecraft in orbit have been developed.^{1,2} The elastic displacement at any arbitrary point in the structure was assumed to result from a superposition of the different flexural modes. The various terms in the general vector equations of motion were expanded in terms of the spatially dependent modal shape functions and frequencies.^{1,2} As a specific example, the dynamics and stability of a long, flexible beam constrained to move only in the orbital plane was considered, with the principal emphasis placed on the motion about the nominal earth pointing (local vertical) orientation.² It was observed that for small amplitude pitch and flexural oscillations, the pitch motion was not affected by the elastic modes, and that the elastic motion was coupled to the pitch motion and described by sets of Mathieu equations. The possibility of parametric instability at very low natural elastic frequencies was demonstrated.

The present paper extends the work of Ref. 2 to consider: (1) the motion and stability of the beam about a nominal local horizontal orientation; and (2) the dynamics of free-free homogeneous platforms in orbit with emphasis placed on a circular plate structure.

DEVELOPMENT OF EQUATIONS OF MOTION-BEAMS ORIENTED ALONG THE LOCAL HORIZONTAL

A Uniform Beam in Orbit with its Axis Nominally along the Local Horizontal

Fig. 1 shows a long, thin flexible beam in orbit with its centroidal axis nominally along the local horizontal. The following assumptions are made in deriving the equations of motion: (a) the beam is long and slender with uniform cross section and uniform distribution of mass and stiffness properties; (b) the center of mass of the beam follows a circular orbit; (c) all motions and deformations of the beam are restricted to occur within the orbit plane; (d) there are no constraints on the beam's elastic motion; (e) longitudinal vibrations of the beam are negligible in comparison to the transverse vibrations.

Based on assumption (c), the Euler angles representing the out-of-plane beam roll and yaw motions vanish and also the out-of-plane component, $\phi_y^{(n)}$, of the mode shape vector is set to zero. In addition as a result of assumption (e) the longitudinal component, $\phi_z^{(n)}$, of the modal shape vector also vanishes. Furthermore, for unconstrained structures and by virtue of the orthogonality conditions together with the other assumptions, it can be shown that both the inertia and gravitational coupling terms between the rigid body modes and flexible modes ($\sum \bar{Q}^{(n)}$, $\sum \bar{G}^{(n)}$, \bar{Q}_n , g_n) appearing in the rotational equations of motion and the generic modal equations (Eqs. (15) and (17) of Ref. 2) vanish. In addition, the terms associated with the shift in the center of mass ($\sum \bar{D}^{(n)}$ and D_n^1)² also vanish for the assumed unconstrained motion. As a result, the rotational and generic equations of motion, for this application, simplify to:

$$J_y \ddot{\omega}_y = G_{Ry} + C_y \quad (1)$$

$$\ddot{A}_n + \omega_n^2 A_n + (\mathcal{S}_{nn} / M_n) = (g_{nn} + E_n) / M_n \quad (2)$$

where

$$\dot{\omega}_y = \dot{\theta}; \omega_y = \dot{\theta} - \omega_c; \theta = \text{pitch angle}$$

$$\omega_c = \text{orbital angular velocity}$$

$$\omega_n = \text{natural frequency of the } n\text{th elastic mode}$$

$$G_{Ry} = 3\omega_c^2 J_y \sin\theta; \mathcal{S}_{nn} = -\omega_y^2 M_n A_n$$

$$g_{nn} = (3 \cos^2\theta - 1) \omega_c^2 M_n A_n$$

$$J_y = \text{beam pitch axis moment of inertia}$$

$$A_n = n^{\text{th}} \text{ flexural modal amplitude}$$

$$M_n = n^{\text{th}} \text{ modal mass}$$

$$C_y = \text{external torque about the pitch axis}$$

$$E_n = \text{effect of external forces on the } n^{\text{th}} \text{ mode}$$

For small amplitude pitch oscillations of the beam with respect to the local horizontal, $\sin\theta \approx \theta$, $\cos\theta \approx 1$, and Eqs. (1) and (2) simplify to,

$$\theta'' - 3\theta = C_y / J_y \omega_c^2 \quad (3)$$

$$\varepsilon_n'' + [(\omega_n / \omega_c)^2 - (\theta' - 1)^2 - 2] \varepsilon_n = E_n / M_n \omega_c^2 \quad (4)$$

where

$$\varepsilon_n = A_n / \ell \quad (\ell = \text{undeformed beam length})$$

$$(\)' = d/d\tau, \text{ where } \tau = \omega_c t$$

$$t = \text{time}$$

It is well known that in the absence of external control torques, the nominal local horizontal orientation of the beam represents an unstable motion which is reflected by Eq. (3). In order to overcome the destabilizing effect of the gravity-gradient torque on the beam, one can either apply active control torques, or adjust the moment of inertia distribution of the system such that the gravity-gradient torque now becomes stabilizing. The beam can be gravitationally stabilized by using a rigid lightweight dumbbell with proper moment of inertia (Fig. 1). In this work the dumbbell is assumed to be attached at the center of the beam by a spring loaded hinge with viscous rotational damping also assumed to be present. The proper moment of inertia of the dumbbell can be attained by selection of the tip masses which are assumed to be much larger than the mass of the dumbbell rod.

Gravitationally Stabilized Flexible Beam in Orbit-Axis Nominally along the Local Horizontal

In addition to the assumptions made in the development of Eqs. (1) - (4), it will also be assumed that the stabilizing dumbbell is rigid and that the mass of the connecting link is negligible compared with that of the tip masses. In addition to the restoring torque provided by the spring, it will also be assumed that a linear viscous damping force is also provided at the hinge.

Thus, the resulting restoring and dissipative torque at the hinge can be represented as,

$$C_y = k(\alpha - \sigma - \theta) + c(\dot{\alpha} - \dot{\sigma} - \dot{\theta}) \tag{5}$$

- where
- k = torsional restoring spring constant at the hinge
 - c = viscous damping coefficient
 - α = angle between the dumbbell axis and the local vertical (see Fig. 1)
 - σ = rotation angle of the beam normal at the hinge due to the elastic deformation (Fig. 1).

For small elastic deformations $(\bar{q} = \sum_n A_n \bar{\phi}^{(n)})$,

$$\sigma = \left. \frac{\partial q_x}{\partial z} \right|_{z=0} = \sum_n A_n \left. \frac{\partial \phi_x^{(n)}}{\partial z} \right|_{z=0} \tag{6}$$

and $\dot{\sigma} = \frac{d\sigma}{dt} = \sum_n \dot{A}_n \left. \frac{\partial \phi_x^{(n)}}{\partial z} \right|_{z=0} \tag{7}$

The modal component of the torque, C_y , can be obtained by replacing C_y by an equivalent force system consisting of two forces of equal magnitude but opposite in sign and separated by a small distance. In the limit as the forces are moved closer,

$$E_n = C_y \left. \frac{\partial \phi_x^{(n)}}{\partial z} \right|_{z=0} \tag{8}$$

The pitch and modal equations for the system shown in Fig. 1 are easily obtained by substituting Eqs. (5)-(8), into Eqs. (1) and (2), with the result, in dimensionless form,

$$\theta'' - 3\sin\theta = \bar{k}(\alpha - \theta) + \bar{c}(\alpha' - \theta') - \sum_n (\bar{k}\epsilon_n + \bar{c}\epsilon_n') C_z^{(n)} \tag{9}$$

$$\epsilon_n'' + [(\omega_n/\omega_c)^2 - (\theta' - 1)^2 - 2]\epsilon_n = \{\bar{k}(\alpha - \theta) + \bar{c}(\alpha' - \theta') - \sum_m (\bar{k}\epsilon_m + \bar{c}\epsilon_m') C_z^{(m)}\} C_z^{(n)} J_y / M_n \ell^2 \tag{10}$$

where, $\bar{k} = k/J_y \omega_c^2$; $\bar{c} = c/J_y \omega_c$

$$C_z^{(n)} = \ell \left. \frac{\partial \phi_x^{(n)}}{\partial z} \right|_{z=0}$$

The equation of motion of the dumbbell is given by,

$$\alpha'' + 3s \sin \alpha = -\bar{k} c_1 (\alpha - \theta) - \bar{c} c_1 (\alpha' - \theta') + \sum_n (\bar{k} \epsilon_n + \bar{c} \epsilon_n') c_1 C_z^{(n)} \quad (11)$$

where,

$$c_1 = J_y / I_d$$

I_d = pitch moment of inertia of the dumbbell.

The following observations can be made from a study of Eqs. (9)-(11): (a) the pitch motion of the beam, the dumbbell motion (α), and the elastic motion of the beam (ϵ_n) are all coupled to each other; (b) within the linear range the elastic modes for which $C_z^{(n)} = 0$ (the symmetric modes), are completely independent of the pitch and dumbbell motions. Furthermore, these modes do not influence either the pitch or dumbbell motion; (c) because of the presence of the dumbbell the natural frequencies and the mode shapes of the symmetric modes of the beam differ from those of the free-free beam. The frequencies and mode shapes can be easily obtained by replacing the dumbbell by a concentrated mass, equal to that of the dumbbell, at the center of the beam.³

STABILITY ANALYSIS - BEAM WITH STABILIZING DUMBBELL

For small amplitude pitch and dumbbell oscillations and small deformations, Eqs. (9)-(11) can be linearized to yield the following equations:

$$\theta'' + \bar{c} \theta' + (\bar{k} - 3) \theta - \bar{c} \alpha' - \bar{k} \alpha + \sum_n (\bar{c} \epsilon_n' + \bar{k} \epsilon_n) C_z^{(n)} = 0 \quad (12)$$

$$\alpha'' + c_1 \bar{c} \alpha' + (c_1 \bar{k} + 3) \alpha - c_1 \bar{c} \theta' - c_1 \bar{k} \theta - \sum_n (\bar{c} \epsilon_n' + \bar{k} \epsilon_n) c_1 C_z^{(n)} = 0 \quad (13)$$

$$\epsilon_n'' + (\Omega_n^2 - 3) \epsilon_n - \{ \bar{k} (\alpha - \theta) + \bar{c} (\alpha' - \theta') \} C_z^{(n)} J_y / M_n \ell^2 + \sum_m (\bar{c} \epsilon_m' + \bar{k} \epsilon_m) C_z^{(nm)} = 0. \quad (14)$$

where $C_z^{(mn)} = J_y C_z^{(m)} C_z^{(n)} / M_n \ell^2$; ($m, n = 1, 2, \dots$) and M_n = mass of the beam for all n .⁴

The small amplitude stability of the solutions to Eqs. (12)-(14) is governed by the roots of the characteristic equation. For the independent symmetric modes the system characteristic equation contains the separate factors

$$[s^2 + (\Omega_n^2 - 3)] = 0; \quad \Omega_n = \omega_n / \omega_c \quad (15)$$

for all the symmetric modes. For the remaining anti-symmetric modes the system characteristic equation can be expressed as

$$\begin{vmatrix} s^2 + \bar{c}s + \bar{k} - 3 & -(\bar{c}s + \bar{k}) & (\bar{c}s + \bar{k}) C_z^{(1)} & \dots & (\bar{c}s + \bar{k}) C_z^{(n)} \\ -(\bar{c}s + \bar{k}) c_1 & s^2 + (\bar{c}s + \bar{k}) c_1 + 3 & -(\bar{c}s + \bar{k}) c_1 C_z^{(1)} & \dots & \dots \\ \vdots & \vdots & \vdots & \ddots & \vdots \\ (\bar{c}s + \bar{k}) C_z^{(n)} / 12 & -(\bar{c}s + \bar{k}) C_z^{(n)} / 12 & A_{1n} & \dots & A_{nn} \\ \vdots & \vdots & \vdots & \ddots & \vdots \end{vmatrix} = 0 \quad (16)$$

where,

$$A_{nm} = (\bar{c}s + \bar{k}) C_z^{(nm)}, \quad n \neq m$$

$$A_{nn} = s^2 + (\bar{c}s + \bar{k}) C_z^{(nn)} + \Omega_n^2 - 3$$

If in a particular model only a finite number of elastic modes are considered in the model, then the associated characteristic equation can be easily obtained from Eq. (16) by deleting the rows and columns corresponding to the neglected modes. The stability analysis of a few selected truncated models is presented in the following sections.

The Case of a Rigid Beam

Here it is assumed that $\phi_x^{(n)} \equiv 0$ for all n , and from Eq. (16) the characteristic equation can be obtained by using only those elements contained in the first two rows and the first two columns, as

$$s^4 + (1+c_1)\bar{c}s^3 + (1+c_1)\bar{k}s^2 + 3(1-c_1)\bar{c}s + 3\bar{k}(1-c_1) - 9 = 0 \quad (17)$$

With an application of the Routh-Hurwitz criterion and noting that $c_1 = J_y/I_d > 0$, the following necessary and sufficient conditions for stability result:

$$\bar{c} > 0; \bar{k} > 0; c_1 < 1; \bar{k} > 3/(1-c_1) \quad (18)$$

The condition: $c_1 < 1$, implies that the dumbbell moment of inertia (I_d) should be greater than the beam (pitch axis) moment of inertia. In the limit as the spring stiffness (k) tends to infinity, the characteristic equation for the lower modes approaches:

$$s^2 + 3(1-c_1)/(1+c_1) = 0, \quad (19)$$

the characteristic equation the system would have if the dumbbell were to be rigidly connected to the beam at the center and pitching with it as a single rigid body.

The Case of a Flexible Beam with only the First Anti-Symmetric Mode Included

In this case it is assumed that $\phi_x^{(n)} = 0$ for all $n \neq 2$ ($n = 1$, first elastic mode). The characteristic equation of this truncated model as obtained from Eq. (16) is given by:

$$\begin{vmatrix} s^2 + \bar{c}s + \bar{k} - 3 & -(\bar{c}s + \bar{k}) & (\bar{c}s + \bar{k}) C_z^{(2)} \\ -(\bar{c}s + \bar{k}) c_1 & s^2 + (\bar{c}s + \bar{k}) c_1 + 3 & -(\bar{c}s + \bar{k}) c_1 C_z^{(2)} \\ (\bar{c}s + \bar{k}) C_z^{(2)} / 12 & -(\bar{c}s + \bar{k}) C_z^{(2)} / 12 & A_{2,2} \end{vmatrix} = 0 \quad (20)$$

where $A_{2,2} = s^2 + (\bar{c}s + \bar{k}) C_z^{(2,2)} + \Omega_2^2 - 3$; $\Omega_2 = \omega_2/\omega_c$.

After formal expansion and application of the Routh-Hurwitz necessary conditions for stability involving the sign of each of the coefficients in the characteristic equation, the following necessary conditions for stability must be satisfied:

$$\bar{c} > 0; \bar{k} > (3 - \Omega_2^2) / (1 + c_1 + C_z^{(2,2)})$$

$$\Omega_2^2 > 6c_1 / (1 + c_1); \bar{k} > 9 / \{(1 + c_1)\Omega_2^2 - 6c_1\}$$

$$\Omega_2^2 > 3(C_z^{(2,2)} / (1 - c_1) + 1)$$

$$\bar{k} > 9(\Omega_2^2 - 3) / \{3(\Omega_2^2 - 3)(1 - c_1) - 9 C_z^{(2,2)}\} \quad (21)$$

The Case of a Flexible Beam with More Than One but a Finite Number of Anti-Symmetric Modes in the Model

In this case $\phi_x^{(n)} = 0$, for $n > m$ where m is a finite integer greater than or equal to 4. As the number of modes retained in the model increases, the direct expansion of the determinantal equation, (16), is algebraically complicated, and an alternate algorithm^{5,6} was used to determine the coefficients of the characteristic equation. For the implementation of this algorithm, it is necessary to rewrite Eqs. (12) - (14) in the standard state variable form

$$X' = AX \quad (22)$$

where $X' = [\theta, \alpha, \epsilon_1, \dots, \epsilon_m, \theta', \alpha', \epsilon_1', \dots, \epsilon_m']^T$

The characteristic equation obtained by this algorithm can be solved for the characteristic roots by any of the many algorithms for determining the roots of an algebraic polynomial equation. (In this case an algorithm based on the modified Bairstow^{6,7} method was used.)

NUMERICAL RESULTS - BEAM WITH STABILIZING DUMBBELL

Figure 2 depicts the root loci of the least damped mode with the spring stiffness (\bar{k}) as the varying parameter for increasingly complex models of the beam-dumbbell system. The root loci are symmetric about the real axis and only the portion above the real axis is shown. The upper curve labeled " $\omega_1 \rightarrow \infty$ " corresponds to the case of the rigid beam. It can be noted that as the spring stiffness increases the roots tend toward the imaginary axis. For the rigid beam case, from Ineq. (18), $\bar{k} > 30$ to ensure stability for the value of $c_1 = J_y / I_d = 0.9$ selected.

When the first anti-symmetric mode is included in the model (solid curves in Fig. 2) the locus is obtained by assuming a particular value for ω_1 / ω_c . The following observations can be made:

- (a) with increasing values of the spring stiffness, \bar{k} , the roots of the characteristic equation move toward the imaginary axis;
- (b) the addition of an elastic mode into the model has the effect of moving the entire root locus toward the origin;
- (c) the minimum value of spring stiffness required for stability is increased.

With the further inclusion of the first two and the first three anti-symmetric modes of the beam into the model, it can be noted from Fig. 2 that a further slight deterioration of the stability characteristics results. The minimum value of hinge spring stiffness required for stability is further increased in these cases.

A representative transient response to an initial displacement about the local horizontal is shown in Figure 3. The long time required to completely damp the system oscillations in the lowest frequency mode may be attributed to the fact that the dumbbell inertia is only slightly larger than the beam's pitch axis inertia in this example ($c_1=0.9$). Increasing the dumbbell inertia can be accomplished by increasing the connecting linkage length within certain limits and/or increasing the tip masses at the expense of the overall useful payload. It is thought that the use of an active control system together with the hinged spring damper may prove to be the most efficient way to remove transient motions and also to achieve shape control in all modes.

A THIN, UNIFORM FLAT PLATE IN ORBIT WITH ITS MAJOR SURFACE NOMINALLY IN THE LOCAL HORIZONTAL PLANE

It is known that a flat plate with its surface normal nominally along the local vertical is gravitationally unstable in the absence of external restoring torques. In order to overcome the destabilizing effect of the gravity-gradient torque on the plate, one can either apply active control torques or adjust the moment of inertia distribution of the system such that the gravity-gradient torque now becomes stabilizing. As in the case of the beam, the plate also can be gravitationally stabilized by attaching a rigid, light weight dumbbell of proper moment of inertia at the center of mass of the plate (Fig. 4). The dumbbell is assumed to be attached to the plate by a spring loaded double gimballed joint. Thus the dumbbell possess two degrees of freedom described by the angles γ and δ as shown in Fig. 4. Damping may be assumed to be present at the hinges of the gimball.

The following assumptions are made in deriving the equations of motion for this system shown in Fig. 4: (a) the plate has a constant thickness which is much less than the other characteristic dimensions of the plate. The mass and stiffness properties are uniformly distributed throughout the plate; (b) the center of mass of the plate is moving along a circular orbit in a spherically symmetric gravitational field of the earth; (c) the elastic displacements in the plane of the plate are negligible compared to those normal to the plane of the plate; (d) the plate is completely free (unconstrained); (e) the mass of the rigid link connecting the two tip masses of the dumbbell is negligible compared to the tip masses; (f) the center of mass of the dumbbell coincides with the center of mass of the undeformed plate; (g) the attitude angles and vibration amplitudes are small; (h) there are no external disturbance and control torques.

With the above assumptions one can derive the linearized equations of motion in the following nondimensional form:

$$\psi'' - \Omega_x \psi - (1 + \Omega_x) \phi' = 0 \quad (23)$$

$$\phi'' - 4\phi + 2\psi' - \bar{c}_z \delta' - \bar{k}_z \delta + \sum_n (\bar{c}_z \epsilon'_n + \bar{k}_z \epsilon_n) C_y^{(n)} = 0 \quad (24)$$

$$\theta'' - 3\theta - \bar{c}_y \gamma' - \bar{k}_y \gamma + \sum_n (\bar{c}_y \epsilon'_n + \bar{k}_y \epsilon_n) C_z^{(n)} = 0 \quad (25)$$

$$\epsilon_n'' + (\Omega_n^2 - 3)\epsilon_n - \{ (\bar{c}_y \gamma' + \bar{k}_y \gamma) J_y C_z^{(n)} + (\bar{c}_z \delta' + \bar{k}_z \delta) J_z C_y^{(n)} \} / M_n \ell^2 + \sum_m \{ (\bar{c}_y \epsilon'_m + \bar{k}_y \epsilon_m) C_z^{(nm)} + (\bar{c}_z \epsilon'_m + \bar{k}_z \epsilon_m) C_y^{(mn)} \} = 0 \quad (26)$$

$$\gamma'' + \bar{c}_y(1+c_1)\gamma' + (3+\bar{k}_y(1+c_1))\gamma + 6\theta - (1+c_1)\sum_n(\bar{c}_y\varepsilon_n' + \bar{k}_y\varepsilon_n)C_z^{(n)} = 0 \quad (27)$$

$$\delta'' + \bar{c}_z(1+c_2)\delta' + (4+\bar{k}_z(1+c_2))\delta + 8\phi - 2\psi' - (1+c_2)\sum_n(\bar{c}_z\varepsilon_n' + \bar{k}_z\varepsilon_n)C_y^{(n)} = 0 \quad (28)$$

where, ψ, ϕ, θ = yaw, roll and pitch angles, respectively; $\varepsilon_n = A_n/\ell$; A_n = modal amplitude; M_n = n^{th} modal mass; ℓ = characteristic length (eg. radius of a circular plate or length of the side of a square plate); γ, δ = dumbbell angles; J_x, J_y, J_z = principal moments of inertia of the plate; I_d = principal moment of inertia of the dumbbell; $\Omega_x = (J_z - J_y)/J_x$; k_y, k_z = torsional spring stiffness; c_y, c_z = damping co-efficients; and,

$$c_1 = J_y/I_d; \quad c_2 = J_z/I_d; \quad \bar{k}_y = k_y/J_y\omega_c^2; \quad \bar{k}_z = k_z/J_z\omega_c^2$$

$$\bar{c}_y = c_y/J_y\omega_c; \quad \bar{c}_z = c_z/J_z\omega_c; \quad C_y^{(n)} = \ell \left. \frac{\partial \phi_x^{(n)}}{\partial y} \right|_{y=0, z=0}$$

$$C_z^{(n)} = \ell \left. \frac{\partial \phi_x^{(n)}}{\partial z} \right|_{y=0, z=0}; \quad C_y^{(mn)} = J_y C_y^{(m)} C_y^{(n)} / M_m \ell^2$$

$$C_z^{(mn)} = J_z C_z^{(m)} C_z^{(n)} / M_m \ell^2$$

A study of Eqs. (23) through (28) reveal that: (i) in general, the pitch, roll, yaw, dumbbell angles (γ and δ) and elastic motions of the plate are all coupled to each other; (ii) the elastic modes for which $C_y^{(n)} = 0$ and $C_z^{(n)} = 0$ can neither influence $\psi, \phi, \theta, \gamma$ and δ nor be influenced by them; however, their frequencies and mode shapes are modified by the dumbbell; (iii) the elastic modes for which $C_y^{(n)} = 0$ and $C_z^{(n)} \neq 0$ are not influenced by ψ, ϕ and δ . However, they are directly coupled to θ and γ ; (iv) the elastic modes for which $C_y^{(n)} \neq 0$ and $C_z^{(n)} = 0$ are not influenced by θ and γ ; however, they are directly coupled to ψ, ϕ and δ ; (v) the elastic modes for which neither $C_y^{(n)}$ nor $C_z^{(n)}$ vanish couple $\psi, \phi, \theta, \gamma$ and δ motions; (vi) the natural frequencies and mode shapes of the elastic modes for which the hinge point ($y=0, z=0$) lies on a nodal line, are not affected by the dumbbell.

The stability of the solutions of the Eqs. (23)-(28) to small initial conditions depend on the characteristic roots of the system. Theoretically, the characteristic determinant of Eqs. (23)-(28) is of infinite order. However, if only a finite number of elastic modes of the plate are retained in the model, the characteristic determinant corresponding to the truncated model is of finite order. A stability analysis of a few such truncated models is discussed in the following section.

STABILITY ANALYSIS-PLATE WITH STABILIZING DUMBBELL

The Case of a Rigid Plate

For a rigid plate, $\phi_x^{(n)} = 0$ for all n . Hence, $C_y^{(n)} = 0$ and $C_z^{(n)} = 0$. This results in (ψ, ϕ, δ) and (θ, γ) being independent of each other. The characteristic roots of the system Eqs. (23)-(28) for this case are given by the roots of the following equations:

Roll-yaw and δ motion

$$\begin{vmatrix} s^2 - \Omega_x & -(1 + \Omega_x)s & 0 \\ 2s & (s^2 - 4) & -(\bar{c}_2 s + \bar{k}_2) \\ -2s & 8 & A_{\delta\delta} \end{vmatrix} = 0 \quad (29)$$

Pitch - γ motion

$$\therefore s^4 + \bar{c}_y(1 + c_1)s^3 + \bar{k}_y(1 + c_1)s^2 + 3\bar{c}_y(1 - c_1)s + 3\bar{k}_y(1 - c_1) - 9 = 0$$

$$\text{where, } A_{\delta\delta} = s^2 + (1 + c_2)(\bar{c}_2 s + \bar{k}_2) + 4 \quad (30)$$

From Eq. (29) it can be observed that for plates with, $\Omega_x = 0$ (e.g. square plates, circular plates etc.), the roll-yaw motion tends to be unstable, which is indicated by the double root at the origin of the complex plane. This instability in roll-yaw may be overcome by introducing a slight asymmetry into the plate such that, $|\Omega_x| \ll 1$ but not equal to zero. This may be achieved by placing small concentrated masses at suitable locations on the plate as dictated by the following necessary conditions for stability which are obtained from Eqs. (29)-(30).

$$\bar{c}_y > 0 ; \bar{c}_z > 0 ; c_1 < 1 ; c_2 < (4 - \Omega_x) / (2 - \Omega_x) ; \Omega_x < 0 ; \bar{k}_y > 3 / (1 - c_1) ; \bar{k}_z > 4 / (1 - c_2)$$

Hence, the slight asymmetry introduced by the small concentrated masses should be such that, $\Omega_x < 0$, i.e. $J_z < J_y$.

It is interesting to note that in the limit as $\bar{k}_y \rightarrow \infty$ and $\bar{k}_z \rightarrow \infty$, the characteristic roots corresponding to the low frequency modes of the system tend toward the roots of the following equations,

$$s^4 + \{(1 + c_2)(2 - \Omega_x) + 2\}s^2 / (1 + c_2) + 4\Omega_x(c_2 - 1) / (1 + c_2) = 0 \quad (31)$$

$$\text{and } s^2 + 3(1 - c_1) / (1 + c_1) = 0 \quad (32)$$

Fig. 5 shows the locus of the roots corresponding to the least damped mode of Eq. (29) with \bar{k}_z as the parameter along each curve. As the value of \bar{k}_z is increased, the roots move toward the imaginary axis to the value as given by Eq. (31). Also, we note that with higher values of $|\Omega_x|$, the roll-yaw stability of the system is improved. The locus of the roots corresponding to the least damped mode of Eq. (30) is shown by the solid curve in Fig. 6. Here also we note that as \bar{k}_y is increased, the roots move toward the imaginary axis to the value as given by Eq. (32). The effects of flexibility on the system stability characteristics is considered in the next section.

The Case of a Flexible Circular Plate

In order to investigate the effects of flexibility on the dynamics, we have considered a circular plate in the present paper. It is well known that the elastic mode shapes of a thin, uniform completely free circular plate are characterized by a nodal pattern which consists of nodal diameters and concentric nodal circles centered at the center of the plate. Mathematically these mode shapes are given by,^{8,9}

$$\phi_x^{(n)} = A_{j,p} [J_p(\lambda_{j,p}\zeta) + C_{j,p} I_p(\lambda_{j,p}\zeta)] \cos p(\beta + \beta_0) \quad (33)$$

where, p = number of nodal diameters ($p = 1, 2, \dots$)

j = number of concentric nodal circles ($j = 1, 2, \dots$)

$\lambda_{j,p}$ = the frequency parameter, $(\omega_{j,p}^2 \sqrt{\rho/D})^{1/2}$;

$\omega_{j,p}$ = natural frequency

ρ = mass density

D = flexural rigidity, $Eh^3/12(1-\nu^2)$

h = thickness of the plate; ν = Poisson's ratio

E = Young's modulus

ζ = nondimensionalized radial distance from the center of the plate ($0 \leq \zeta \leq 1$)

β = polar angle measured with respect to the y axis

β_0 = arbitrary phase angle

J_p, I_p = Bessel and modified Bessel functions of the first kind

$A_{j,p}, C_{j,p}$ = constants whose value can be adjusted to yield the modal mass equal to the mass of the plate⁸

Based on Eq. (33) one can easily show that for circular plates,

$$C_y^{(n)} = \begin{cases} \frac{1}{2} A_{j,1} \lambda_{j,1} (1+C_{j,1}) \cos \beta_0 & \text{for } p = 1 \\ 0 & \text{for } p \neq 1 \end{cases} \quad (34)$$

and,

$$C_z^{(n)} = \begin{cases} \frac{1}{2} A_{j,1} \lambda_{j,1} (1+C_{j,1}) \cos (\pi/2 + \beta_0) & \text{for } p = 1 \\ 0, & \text{for } p \neq 1 \end{cases} \quad (35)$$

Thus, Eqs. (23) through (28) are coupled to each other through the elastic modes which have only one nodal diameter. The other elastic modes are independent of $\psi, \phi, \theta, \gamma$ and δ .

In the previous section it was assumed that small concentrated masses were placed on the plate such that, $\Omega_x < 0$ to prevent the instability in the roll-yaw degree of freedom. The concentrated masses are assumed to be placed at the ends of the diameter along the roll axis (z -axis) of the plate. Because of this asymmetry in the plate, the arbitrary phase angle, β_0 , in Eq. (33) can now have the values 0 or $\pi/2$ only.¹⁰ This implies that the nodal diameters can have only one of the following two orientations: (1) a nodal diameter along the roll or z axis of the plate ($\beta_0=0$); and (2) a nodal diameter along the pitch or y -axis of the plate ($\beta_0=\pi/2$). The natural frequency and the mode shapes of the plate are not affected by the concentrated masses for the first orientation of the nodal diameter. However, the small concentrated masses slightly perturb the values of the natural frequencies and the mode shapes of those elastic modes for which the position of the concentrated masses do not lie on a nodal line.

To a first order approximation, the values of the perturbed natural frequency and the perturbed mode shapes are given by,¹⁰

$$\omega_{n_p}^2 \approx \omega_n^2 \left(1 - \frac{\delta M}{M_n} \{\phi_x^{(n)}(\ell)\}^2\right); \quad \frac{\delta M}{M_n} \ll 1$$

$$\phi_{x_p}^{(n)} \approx \phi_x^{(n)} + \sum_{(m \neq n)} \mu_m \phi_x^{(m)} \quad (37)$$

where, ω_{n_p} , $\phi_{x_p}^{(n)}$ = perturbed natural frequency and mode shape

ω_n , $\phi_x^{(n)}$ = unperturbed natural frequency and mode shape

δM = total mass added

$$\mu_m = \frac{\omega_n^2}{\omega_m^2 - \omega_n^2} \frac{\delta M}{M_n} \phi_m(\ell) \phi_n(\ell)$$

In the following sections the dynamics of a flexible circular plate for the previously mentioned two possible orientations of the nodal diameter are discussed separately.

The case of a nodal diameter along the pitch axis or y axis of the plate ($\beta_0 = \pi/2$). For this orientation of the nodal diameter $C_y^{(n)} = 0$ for all n (Eq. (34)). Hence, (ψ, ϕ, δ) motions become completely independent of pitch, γ and elastic motions of the plate and thus the plate behaves like a rigid body in the roll-yaw degree of freedom. However, the θ and γ motions are coupled to the elastic motions of the plate through the terms containing $C_y^{(n)}$ in Eqs. (25)-(27). The stability of the solutions of these equations to small initial conditions is governed by the roots of a characteristic equation which theoretically is an infinite degree polynomial equation. However, in practice since only a finite number of modes are retained in the mathematical model, the degree of this polynomial equation will be finite. A stability analysis of such truncated models is presented in Fig. 6.

It can be noted from Fig. 6 that the characteristic roots corresponding to the least damped mode of the system behave similar to those discussed in Fig. 3.

The case of a nodal diameter along the roll axis or z axis of the plate ($\beta_0 = 0$). For this orientation of the nodal diameter $C_z^{(n)} = 0$ for all n (Eq. (35)). Hence, (θ, γ) motions become completely independent of ψ, ϕ, δ and elastic motions of the plate and thus the plate behaves like a rigid body in the pitch degree of freedom. However, ψ, ϕ, δ are coupled to the elastic motions of the plate through the terms containing $C_y^{(n)}$ in Eqs. (23), (24), (26) and (28). A parametric study of the least damped mode characteristics for these equations results in a root locus plot similar to those presented in Figs. 2 and 6.

CONCLUSIONS

Space structures with their maximum moment of inertia axis along the local vertical are gravitationally unstable. Such structures may be gravitationally stabilized by attaching a light weight dumbbell with heavy tip masses.

An analysis of the dynamics of two such systems, a thin flexible beam nominally along the local horizontal and a flat plate with its surface normal nominally along the local vertical, is presented in this paper.

In the case of the flexible beam, the dumbbell motion excites only the anti-symmetric elastic modes of the beam. However, the frequencies and the mode shapes of the symmetric modes of the beam are modified by the presence of the dumbbell.

For case of flat circular plates, the dumbbell can excite only those elastic modes with only one nodal diameter. Also, the dumbbell modifies the value of natural frequency and mode shapes of axi-symmetric modes of the plate. The small concentrated masses added to the plate for roll-yaw stability results in only two possible orientations for the nodal diameters. These concentrated masses slightly perturb the value of the natural frequency and mode shapes, if they do not lie on a nodal line.

For all the cases presented in this paper, the characteristic roots corresponding to the least damped mode of the system move toward the imaginary axis as the torsional spring stiffness at the hinge is increased. The stability of the truncated model deteriorates with the increase in the number of elastic modes retained in the model.

In order to damp the motion of the system in all its modes, especially the low frequency modes, the use of active dampers (control systems) are needed. However, it is thought that with the use of the passive gimballed dumbbell stabilization device together with active controllers, both the peak forces as well as fuel consumption could be significantly reduced. Such a study would represent a logical extension of the present paper.

ACKNOWLEDGEMENT

Research supported by NASA Grant NSG-1414, Suppl. 2, Mr. H.A. Hamer, NASA-Langley Research Center, Technical Officer.

REFERENCES

1. Santini, Paolo, "Stability of Flexible Spacecrafts," Acta Astronautica, Vol. 3, 1976, pp. 685-713.
2. Kumar, V.K., and Bainum, P.M., "Dynamics of a Flexible Body in Orbit," AIAA/AAS Astrodynamics Conference, Palo Alto, Calif., August 7-9, 1978, Paper No. 78-1418; also J. of Guidance and Control, Vol. 3, Jan. - Feb. 1980, pp. 90-92 (Engineering Note).
3. Bisplinghoff, R.L. and Ashley, H., Principles of Aeroelasticity, Dover Publication, Inc., New York, 1962, pp. 80-84.
4. Eishop, R.E.D., and Johnson, D.C., The Mechanics of Vibration, Cambridge, University Press, 1960, p. 323.
5. Zadeh, L.A. and Desoer, C.A., Linear System Theory, McGraw Hill Book Co., New York, 1963, pp. 303-305.
6. Melsa, J.L. and Jones, S.K., Computer Programs for Computational Assistance in the Study of Linear Control Theory, McGraw Hill Book Co., New York, 1970, pp. 6-11.
7. Hamming, R.W., Numerical Methods for Scientists and Engineers, McGraw-Hill Book Co., Inc., New York, 1962, pp. 356-359.
8. Liessa, A.W., "Vibration of Plates," NASA SP-160, (NASA, Washington, D.C.) 1969, pp. 7-35.

9. Itao, K. and Crandall, S.H., "Natural Modes and Natural Frequencies of Uniform, Circular, Free-Edge Plates," J. of Appl. Mech., Trans. of the ASME, Vol. 46, June 1979, pp. 448-453.
10. Rayleigh, Lord, The Theory of Sound, Vol. I, Dover Pub., New York, 1945, pp. 113-119, 363-367.

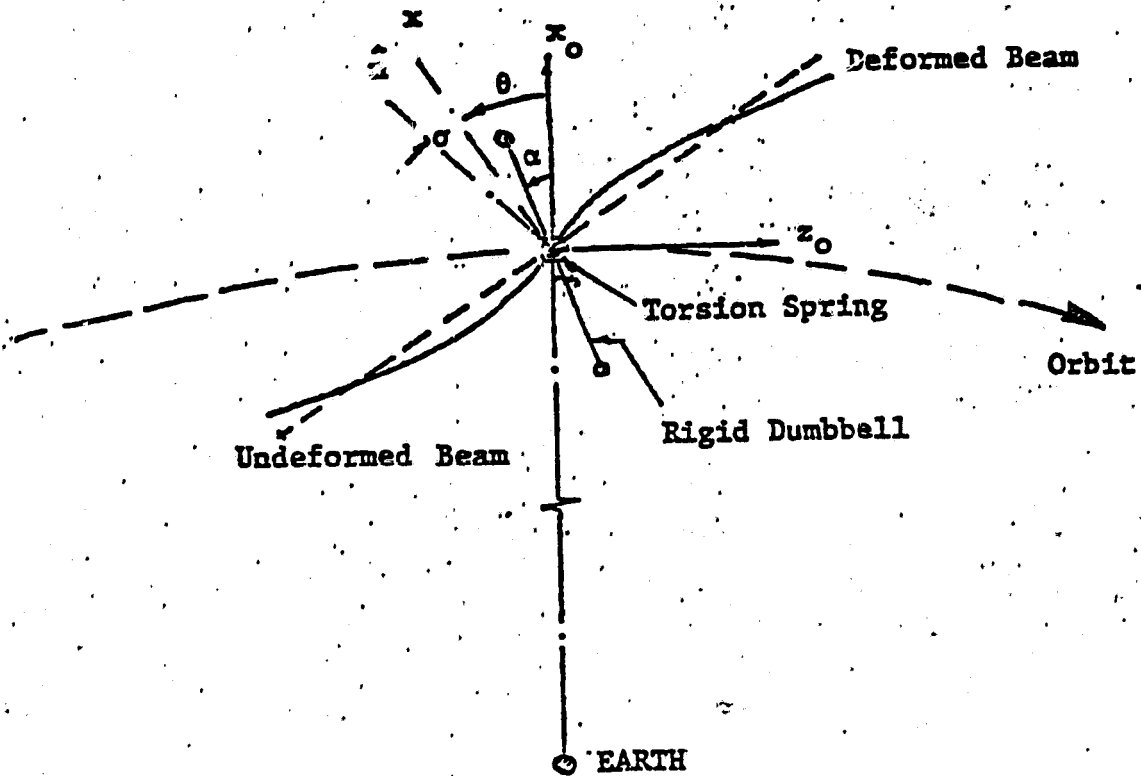


Fig. 1: Dumbbell Stabilized Flexible Beam With Nominal Orientation Along Local Horizontal

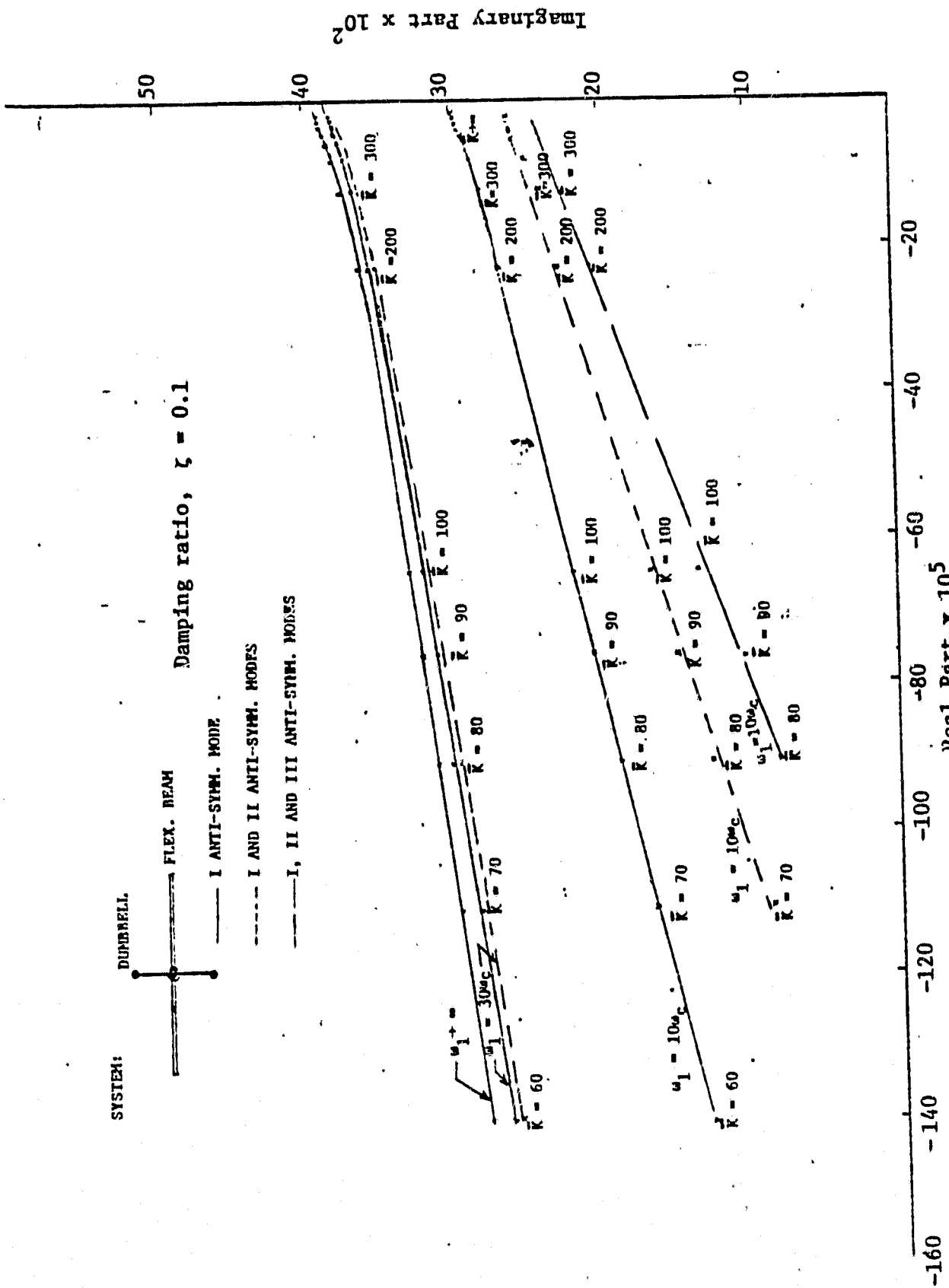


Fig. 2: Variations in Root Loci of the Least Damped Mode with Beam Stiffness and Dumbbell Restoring Characteristics

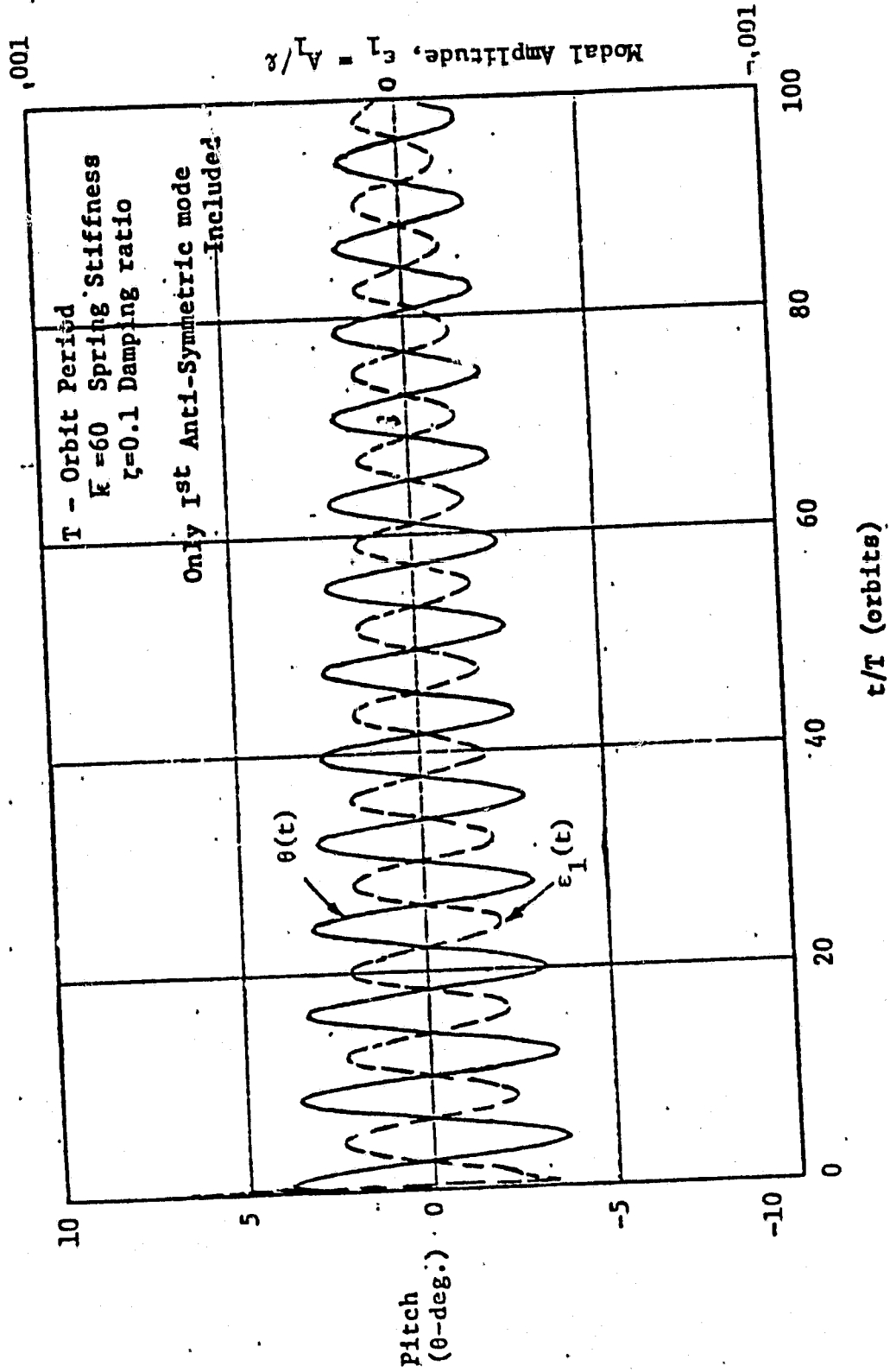


Fig. 3: Time Response of Dumbbell Stabilized Flexible Beam in Orbit.

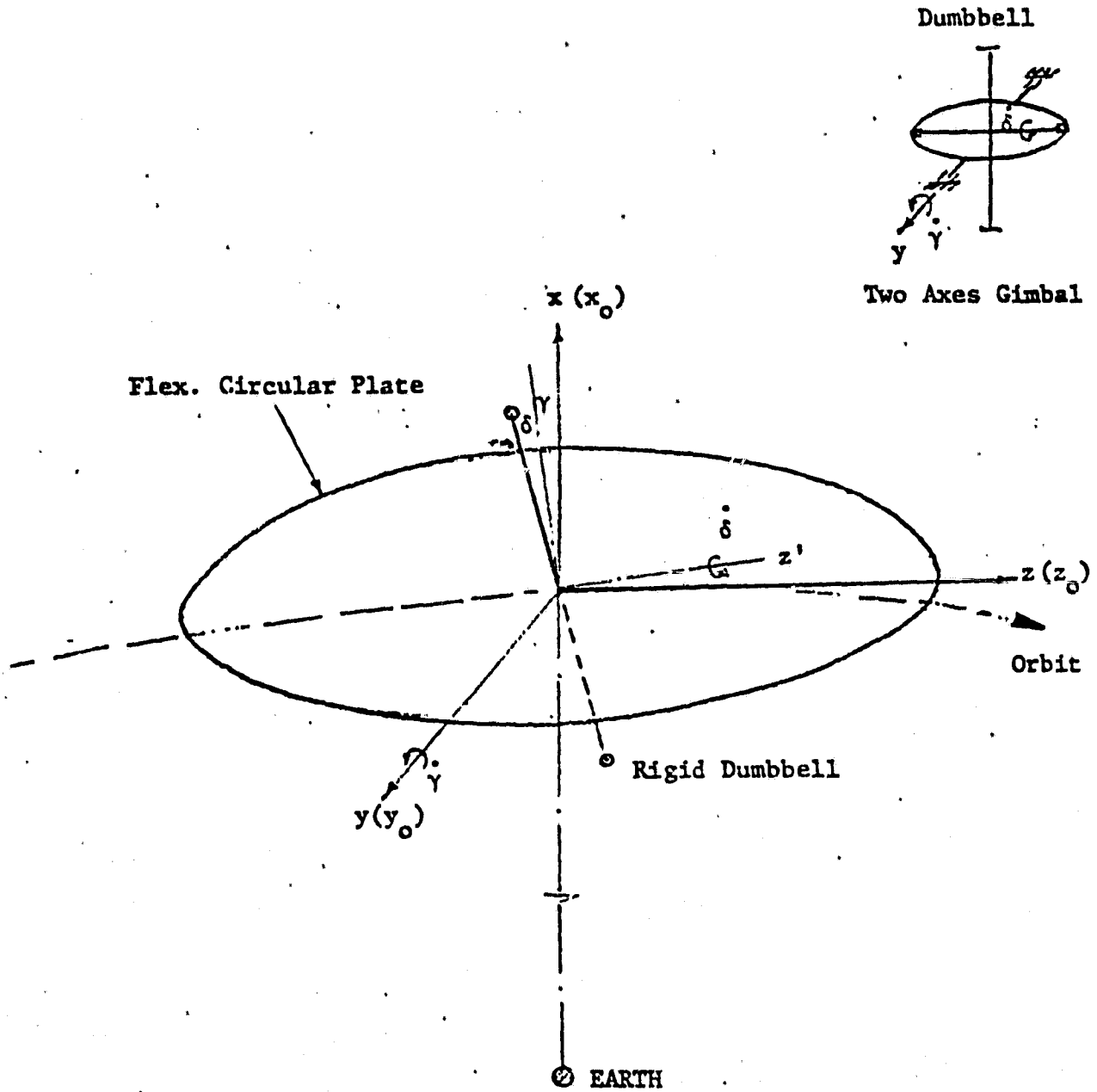


Fig. 4: Flexible Circular Plate Nominally in the Local Horizontal Plane with the Stabilizing Dumbbell.

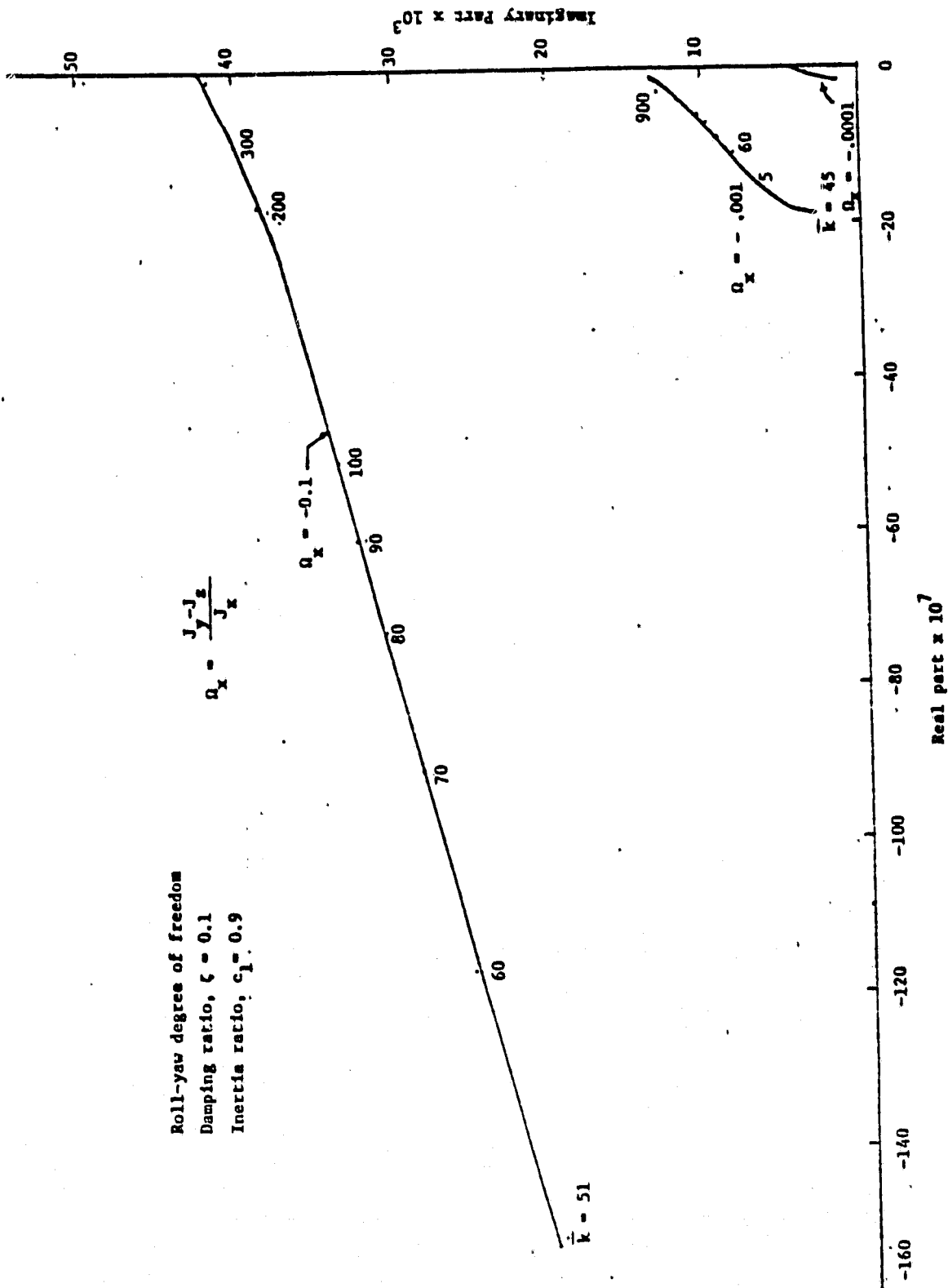


Fig. 5: Root Locus of Least Damped Mode - Rigid Circular Plate with Dumbbell

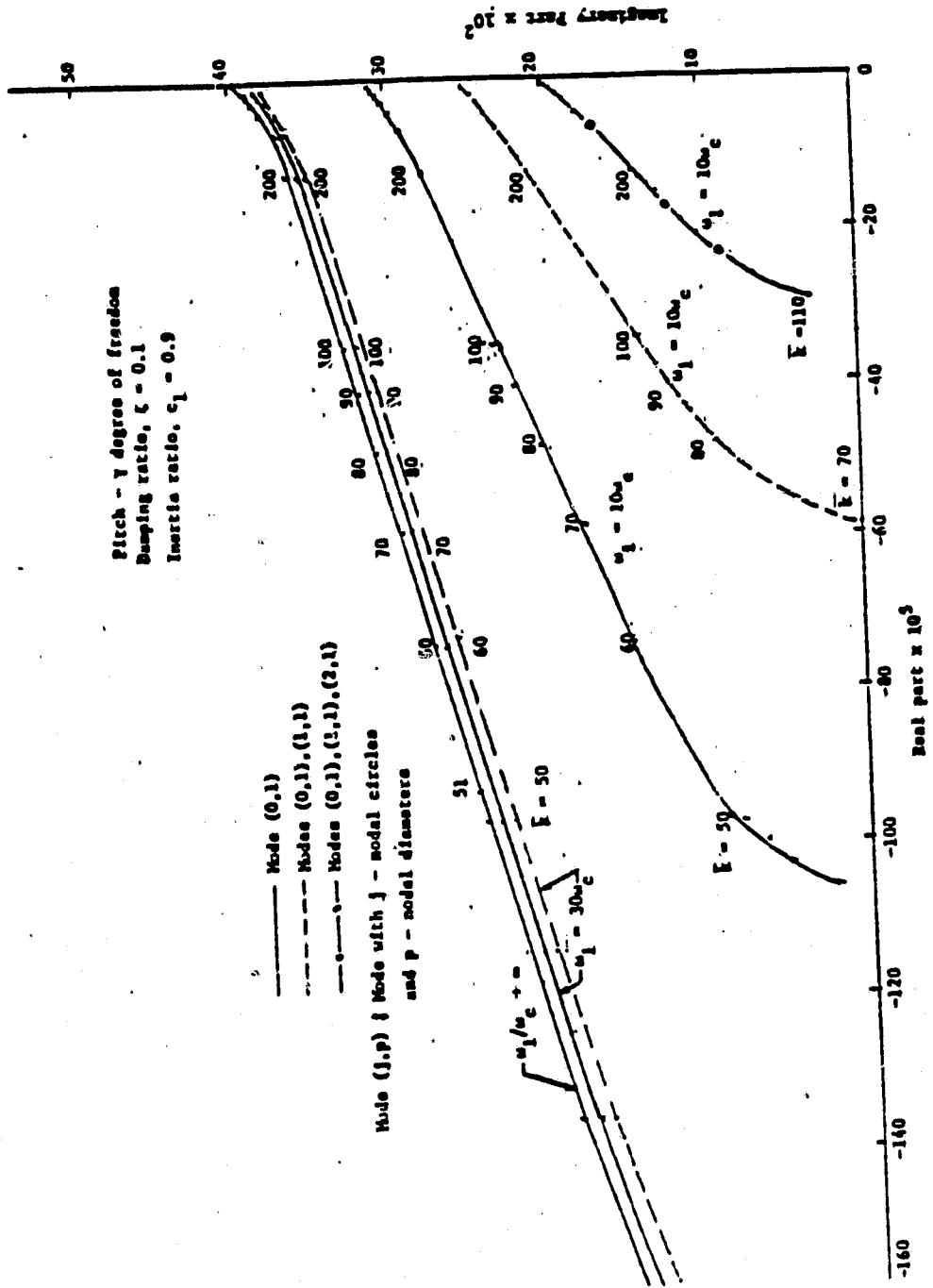


Fig. 6: Root Locus of Least Damped Mode - Circular Plate with Dumbbell (Nodal Diameter Along Pitch Axis)

Chapter 4

ON THE MOTION OF A FLEXIBLE SHALLOW SPHERICAL SHELL IN ORBIT

In this chapter an analysis of the motion of a thin, shallow spherical shell type structure in orbit nominally pointing towards the earth along the local vertical is presented. It is known that in this orientation, the system is gravitationally unstable. Such structures may be passively stabilized with a connecting dumbbell. Hence an analysis of the motion of a shell structure with a stabilizing dumbbell is also presented in this chapter.

DEVELOPMENT OF EQUATIONS OF MOTION-SHELL AXIS ORIENTED ALONG THE LOCAL VERTICAL

Fig. 4.1a shows a shallow spherical shell with the various notations defined. The assumptions that were made in deriving the model for the shell are as follows:

- (i) the mass and elastic properties are distributed continuously and uniformly throughout the domain of the shell;
- (ii) the thickness of the shell is small as compared to the height of the shell;
- (iii) the ratio, height (H)/base radius (ℓ) is much less than unity (condition for shallowness);
- (iv) the edge of the shell is completely free;
- (v) the elastic deformations perpendicular to the symmetry axis (i.e. x-axis) of the shell are negligible compared to the deformations parallel to the symmetry axis, i.e. only transverse vibrations are considered;
- (vi) the center of mass of the shell is moving in a circular orbit.

The transverse vibrational mode shapes of shallow shells can be conveniently expressed in a cylindrical system of co-ordinates (r_c, β, x_c) can be related to the x_c, y_c, z_c system (see Fig. 4.1a).^{1,2}

In order to evaluate the coupling terms in Eqs. (2.5) and (2.14) for the present case, let us express, $r_0 = r_1 + r_2$ (4.1)

where, \bar{r}_1 = the vector from the center of mass of the shell to the origin of (x_c, y_c, z_c)

\bar{r}_2 = the vector from the origin of (x_c, y_c, z_c) to a generic point on the shell.

Since the shell is assumed to be completely free, by Eqs. (2.16) and (2.17) we have,

$$\begin{aligned} \int_v \bar{q} \, dm &= 0 \\ \int_v \dot{\bar{q}} \, dm &= 0 \\ \int_v \bar{r}_0 \times \ddot{\bar{q}} \, dm &= 0 \end{aligned} \quad (4.2)$$

Using Eqs. (4.1) and (4.2) in Eqs. (2.5)-(2.14) one can easily show that,

$$\begin{aligned} \sum_n \bar{Q}^{(n)} &= \int_v [2\bar{r}_2 \times (\bar{\omega} \times \bar{q}) + \bar{r}_2 \times (\dot{\bar{\omega}} \times \bar{q}) + \bar{q} \times (\dot{\bar{\omega}} \times \bar{r}_2) - (\bar{r}_2 \cdot \bar{\omega}) (\bar{\omega} \times \bar{q}) \\ &\quad - (\bar{q} \cdot \bar{\omega}) (\bar{\omega} \times \bar{r}_2)] \, dm \end{aligned} \quad (4.3)$$

$$\sum_n \bar{G}^{(n)} = \int_v (\bar{r}_2 \times M^{(c)} \bar{q} + \bar{q} \times M^{(c)} \bar{r}_2) \, dm \quad (4.4)$$

$$\bar{\mathcal{P}}_n = \int_v [\bar{\phi}^{(n)} \cdot \bar{\omega} \times \bar{r}_2 + \dot{\bar{\phi}}^{(n)} \cdot \bar{\omega} \times (\bar{\omega} \times \bar{r}_2)] \, dm \quad (4.5)$$

$$\sum_m \bar{\mathcal{P}}_{mn} = \int_v \bar{\phi}^{(n)} \cdot \bar{\omega} \times (\bar{\omega} \times \bar{q}) \, dm \quad (4.6)$$

$$\bar{g}_n = \int_v \bar{\phi}^{(n)} \cdot M^{(c)} \bar{r}_2 \, dm \quad (4.7)$$

$$\sum_m \bar{g}_{mn} = \int_v \bar{\phi}^{(n)} \cdot M^{(c)} \bar{q} \, dm \quad (4.8)$$

where, $M^{(c)} = T_4 M T_4^{-1}$

T_4 = transformation matrix given by Eq. (A.2)

M = matrix operator given by Eq. (A.4)

In deriving Eq. (4.6) use has been made of the assumption that the elastic deformations are parallel to the symmetry axis only, i.e. $\bar{q} = |\bar{q}| \hat{i}$.

The following observations can be made from Eqs. (4.4)-(4.8);

- (a) the rigid body rotational mode and elastic modes of the shell are coupled to each other by both inertia and gravity;
- (b) the earth's gravitational field can excite elastic motion in the shell through rigid body coupling terms.

After expressing the various vectors in Eqs. (4.4)-(4.8) in the cylindrical co-ordinate system (r_c, β, x_c) we have,

$$\bar{r}_2 = r_c \hat{e}_r + x_c \hat{i} \quad (4.9)$$

$$\begin{aligned} \bar{\omega} &= \omega_r \hat{e}_r + \omega_\beta \hat{e}_\beta + \omega_x \hat{i} \\ &= \omega_x \hat{i} + \omega_y \hat{j} + \omega_z \hat{k} \end{aligned} \quad (4.10)$$

$$\bar{q} = \sum_n A_n(t) \phi_x^{(n)}(r_c, \beta) \quad (4.11)$$

$$\phi_x^{(n)} = \phi_x^{(n)} \hat{i} \quad (4.12)$$

By substituting Eqs. (4.9)-(4.12) into Eqs. (4.3)-(4.8) one obtains

$$\begin{aligned} \bar{Q}^{(n)} &= \int_V 2\dot{A}_n \{x_c (\dot{\bar{\omega}} - \dot{\omega}_x \hat{i}) - r_c \dot{\omega}_r \hat{i}\} \\ &\quad + A_n \{x_c (\ddot{\bar{\omega}} - \ddot{\omega}_x \hat{i}) - r_c \ddot{\omega}_r \hat{i}\} \\ &\quad + A_n \{x_c (\ddot{\bar{\omega}} - \ddot{\omega}_x \hat{i}) - r_c \ddot{\omega}_x \hat{e}_r\} \\ &\quad - A_n (r_c \dot{\omega}_r + x_c \dot{\omega}_x) (\omega_z \hat{j} - \omega_y \hat{k}) \\ &\quad - A_n \omega_x \{(\omega_\beta x_c \hat{e}_r - (\omega_r x_c - r_c \omega_x) \hat{e}_\beta - r_c \omega_\beta \hat{i})\} \phi_x^{(n)} dm \end{aligned} \quad (4.13)$$

$$\begin{aligned} \bar{G}^{(n)} &= A_n \int_V \phi_x^{(n)} [r_c M_{31}^{(c)} \hat{i} - x_c M_{31}^{(c)} \hat{e}_r + (x_c M_{21}^{(c)} - r_c M_{11}^{(c)}) \hat{e}_\beta \\ &\quad + (x_c M_{21}^{(c)} + r_c M_{22}^{(c)}) \hat{e}_\beta - (x_c M_{31}^{(c)} + r_c M_{32}^{(c)})] dm \end{aligned} \quad (4.14)$$

$$\bar{\Phi}_n = - \int_V \{r_c \dot{\omega}_\beta + x_c (\omega_y^2 + \omega_z^2) - r_c \omega_x \omega_r\} \phi_x^{(n)} dm \quad (4.15)$$

$$\bar{\Phi}_{mn} = -A_m (\omega_y^2 + \omega_z^2) \delta_{mn} M_n \quad (4.16)$$

$$\bar{g}_n = \int_V (M_{11}^{(c)} x_c + M_{12}^{(c)} r_c) \phi_x^{(n)} dm \quad (4.17)$$

$$\begin{aligned}
\bar{G}^{(n)} = & A_n \{ \{ M_{21} I_3^{(n)} + M_{31} I_2^{(n)} \} \hat{i} \\
& + \{ -2M_{21} I_5^{(n)} - 2M_{31} I_4^{(n)} + M_{11} I_3^{(n)} - M_{23} I_6^{(n)} \\
& - \frac{M_{22}}{2} (I_7^{(n)} + I_3^{(n)}) + \frac{M_{33}}{2} (I_7^{(n)} - I_3^{(n)}) \} \hat{j} \\
& + \{ 2M_{21} I_4^{(n)} - 2M_{31} I_5^{(n)} - M_{23} I_7^{(n)} + \frac{M_{22}}{2} (I_6^{(n)} + I_2^{(n)}) \\
& - \frac{M_{33}}{2} (I_6^{(n)} - I_2^{(n)}) \} \hat{k}] \quad (4.22)
\end{aligned}$$

$$\mathcal{Q}_n = \dot{\omega}_y I_3^{(n)} - \dot{\omega}_z I_2^{(n)} - (\omega_y^2 + \omega_z^2) I_1^{(n)} + \omega_x \omega_y I_2^{(n)} + \omega_x \omega_z I_3^{(n)} \quad (4.23)$$

$$\mathcal{Q}_{mn} = -A_m (\omega_y^2 + \omega_z^2) \delta_{mn} M_n \quad (4.24)$$

$$\mathcal{E}_n = M_{11} I_1^{(n)} + M_{21} I_2^{(n)} - M_{31} I_3^{(n)} \quad (4.25)$$

$$\mathcal{E}_{mn} = A_m M_{11} \delta_{mn} M_n \quad (4.26)$$

where,

$$\begin{aligned}
I_1^{(n)} &= \int_V x_c \phi_x^{(n)} dm; & I_2^{(n)} &= \int_V r_c c \beta \phi_x^{(n)} dm; & I_3^{(n)} &= \int_V r_c s \beta \phi_x^{(n)} dm; \\
I_4^{(n)} &= \int_V x_c s 2\beta \phi_x^{(n)} dm; & I_5^{(n)} &= \int_V x_c s 2\beta \phi_x^{(n)} dm; & I_6^{(n)} &= \int_V r_c c 3\beta dm; \\
I_7^{(n)} &= \int_V r_c s 3\beta dm
\end{aligned}$$

Since, the shell is assumed to be completely free, the mode shapes satisfy the condition in Eq. (2.17).

i.e.

$$\int_V \bar{r}_0 x \phi^{(n)} dm = 0$$

With $\bar{r}_0 = \bar{r}_1 + \bar{r}_2$ and $\phi^{(n)} = \phi_x^{(n)} \hat{i}$, Eq. (2.17) translates into,

$$\int_V \bar{r}_2 x \phi_x^{(n)} \hat{i} dm = 0$$

i.e.

$$-I_3^{(n)} \hat{j} + I_2^{(n)} \hat{k} = 0$$

Hence, $I_2^{(n)} \equiv 0$ (4.27)

$I_3^{(n)} \equiv 0$ (4.28)

The mode shapes of a completely free shallow spherical shell are characterized by a nodal pattern consisting of a set of j concentric nodal circles centered on the symmetry axis and p nodal diameters. The mode shape as given by Eq. (B.4) in Appendix - B is in the form

$$\phi_x^{(n)} = W_{j,p}(\zeta) \cosp(\beta + \beta_0) \quad (4.29)$$

where, $\zeta = r_c / \ell$ and $\ell =$ the base radius of the shell .

Using the form of $\phi_x^{(n)}$ in Eq. (4.29) we can evaluate the integrals, $I_1^{(n)}$ through $I_7^{(n)}$ as follows:

$$\begin{aligned} I_1^{(n)} &= \int_V x_c \phi_x^{(n)} dm \\ &= \rho \ell^2 \int_0^1 \int_0^{2\pi} x_c(\zeta) W_{j,p}(\zeta) \cosp(\beta + \beta_0) \zeta d\zeta d\beta \end{aligned}$$

i.e., $I_1^{(n)} = 2m \delta_{op} I_{x_0}^{(j)}$ (4.30)

where, $I_{x_0}^{(j)} = \int_0^1 x_c(\zeta) W_{j,0}(\zeta) \zeta d\zeta$

$m =$ mass of the shell, $\pi \rho \ell^2$

$$\delta_{op} = \begin{cases} 1, & p = 0 \\ 0, & p \neq 0 \end{cases}$$

Now consider,

$$\begin{aligned} I_4^{(n)} &= \int_V x_c c2\beta \phi_x^{(n)} dm \\ &= \rho \ell^2 \int_0^1 \int_0^{2\pi} x_c(\zeta) W_{j,p}(\zeta) \cosp(\beta + \beta_0) \cos 2\beta \zeta d\zeta d\beta \end{aligned}$$

i.e. $I_4^{(n)} = m \cosp\beta_0 \delta_{2p} I_{x_2}^{(j)}$ (4.31)

Similarly,

$$I_5^{(n)} = -m \sin p\beta_0 \delta_{2p} I_{x_2}^{(j)} \quad (4.32)$$

$$I_6^{(n)} = m\ell \cos p\beta_0 \delta_{3p} I_r^{(j)} \quad (4.33)$$

$$I_7^{(n)} = -m\ell \sin p\beta_0 \delta_{3p} I_r^{(j)} \quad (4.34)$$

where, $I_{x_2}^{(j)} = \int_0^1 x_c(\zeta) W_{j,2}(\zeta) \zeta d\zeta$

$$I_r^{(j)} = \int_0^1 \zeta^2 W_{j,3}(\zeta) d\zeta$$

$$\delta_{kp} = \begin{cases} 1, & p=k \\ 0, & p \neq k \end{cases} \quad (k=2,3)$$

The integrals $I_{x_0}^{(j)}$, $I_{x_2}^{(j)}$ and $I_r^{(j)}$ are evaluated in Appendix C. Their values are given by,

$$I_{x_0}^{(j)} = 2A_{j,0} \frac{\ell^2}{R} (1+\nu) J_1(\lambda_{j,0}) / \lambda_{j,0}^3 \quad (4.35)$$

$$I_{x_2}^{(j)} = \frac{\ell^2}{2R} A_{j,2} \left[\frac{\ell^6}{12RD\lambda_{j,2}^4} C_{j,2} + \frac{D_{j,2}}{\lambda_{j,2}^3} \{2\lambda_{j,2} (I_0(\lambda_{j,2})+1) - 8I_1(\lambda_{j,2})\} \right. \\ \left. + \frac{1}{\lambda_{j,2}^3} \{2\lambda_{j,2} (J_0(\lambda_{j,2})+1) - 8J_1(\lambda_{j,2})\} \right] \quad (4.36)$$

$$I_r^{(j)} = \frac{\ell^3}{6RD\lambda_{j,3}^4} C_{j,3} + \frac{1}{\lambda_{j,3}^3} \{8 - 8J_0(\lambda_{j,3}) - 4\lambda_{j,3} J_1(\lambda_{j,3}) - \lambda_{j,3}^2 J_2(\lambda_{j,3})\} \\ + \frac{D_{j,3}}{\lambda_{j,3}^3} \{\lambda_{j,3}^2 I_2(\lambda_{j,3}) - 4\lambda_{j,3} I_1(\lambda_{j,3}) + 8I_0(\lambda_{j,3}) - 8\} \quad (4.37)$$

where, ν = Poisson's ratio

$A_{j,p}, C_{j,p}, D_{j,p}$ = constants in the mode shape function in Eq. (C.4) ($j, p = 1, 2, \dots$)

After substituting Eqs. (4.21)-(4.28) into Eqs. (2.2) and (2.3), we arrive at Eqs. (4.38) - (4.41) for the motion of the shallow shell in orbit.

$$\text{Yaw: } \dot{\omega}_x + \Omega_x \omega_y \omega_z = \Omega_x M_{23} + C_x / J_x \quad (4.38)$$

$$\begin{aligned} \text{Pitch: } \dot{\omega}_y + \Omega_y \omega_z \omega_x + 2 \sum_n (\dot{A}_n \omega_y + A_n \dot{\omega}_y - A_n \omega_z \omega_x) \frac{I_1^{(n)}}{J_y} \\ = \Omega_y M_{31} + \sum_n \left\{ \frac{1}{2} (M_{33} - M_{22}) I_7^{(n)} - 2M_{21} I_5^{(n)} - (2M_{31} I_4^{(n)} + M_{23} I_6^{(n)}) \right\} \frac{A_n}{J_y} + \frac{C_y}{J_z} \end{aligned} \quad (4.39)$$

$$\begin{aligned} \text{Roll: } \dot{\omega}_z + \Omega_z \omega_x \omega_y + 2 \sum_n (\dot{A}_n \omega_z + A_n \dot{\omega}_z + A_n \omega_x \omega_y) \frac{I_1^{(n)}}{J_z} \\ = \Omega_z M_{12} + \sum_n \left\{ \frac{1}{2} (M_{22} - M_{33}) I_6^{(n)} + 2M_{21} I_4^{(n)} - (2M_{31} I_5^{(n)} + M_{23} I_7^{(n)}) \right\} \frac{A_n}{J_z} + C_z / J_z \end{aligned} \quad (4.40)$$

$$\text{Modes: } \ddot{A}_n + \omega_n^2 A_n - (\omega_y^2 + \omega_z^2) \frac{I_1^{(n)}}{M_n} - (\omega_x^2 + \omega_z^2) A_n = M_{11} \frac{I_1^{(n)}}{M_n} + M_{11} A_n + \frac{E_n}{M_n} \quad (4.41)$$

$$\text{where, } \Omega_x = (J_z - J_y) / J_x ; \Omega_y = (J_x - J_z) / J_y ; \Omega_z = (J_y - J_x) / J_z ;$$

$$\Omega_n = \omega / \omega_c ; \epsilon_n = A_n / \ell ; \ell = \text{base radius of the shell;}$$

In order to examine the stability of the system response to small initial conditions, Eqs. (4.38)-(4.41) are linearized assuming small amplitude pitch (θ), roll (ϕ), yaw (ψ) and elastic displacements (A_n) and denoting $\frac{d}{d\tau} () = ()'$; $\tau = \omega_c t$.

As a result of this we arrive at the following linear equations of motion for the shallow shell:

$$\psi'' - \Omega_x \psi - (1 + \Omega_x) \phi' = C_x / J_x \omega_c^2 \quad (4.42)$$

$$\phi'' + 4\Omega_z \phi + (1 - \Omega_z) \psi' = C_z / J_z \omega_c^2 \quad (4.43)$$

$$\theta'' - 3\Omega_y \theta - 2 \sum_n \epsilon_n' I_1^{(n)} \ell / J_y = C_y / J_y \omega_c^2 \quad (4.44)$$

$$\epsilon_n'' + (\Omega_n^2 - 3) \epsilon_n + 2\theta' I_1^{(n)} / M_n \ell = 3I_1^{(n)} / M_n \ell + E_n / M_n \omega_c^2 \ell \quad (4.45)$$

An examination of Eqs. (4.42) - (4.45) reveals the following points (external disturbance assumed to be zero):

- in the linear range of operation, the motion in the roll-yaw degree of freedom can be studied independently of the pitch and elastic motions;
- the pitch and elastic motions are coupled directly to each other through their rates;
- since $I_1^{(n)} = 0$ for all elastic modes except for the axi-symmetric modes (i.e. modes with no nodal diameters), only axi-symmetric modes are responsible for the coupling of pitch and the elastic motions. Non-axisymmetric modes are independent of the rigid body rotational motions, ψ, ϕ , and θ ;

- the axisymmetric elastic modes are subjected to a constant excitation force due to the orbital motion and gravity effects;
- the pitch and the roll-yaw motions are unstable about the present nominal orientation because of the unfavorable moment of the inertia distribution.

In order to stabilize the pitch motion, a passive stabilization procedure using a light weight dumbbell, as proposed in the case of flat plate, is also considered in the next section.

GRAVITATIONALLY STABILIZED SHALLOW SHELL IN ORBIT

A gravitationally stabilized shallow spherical shell in a circular orbit is shown in Fig. 4.1b. The stabilizing dumbbell is assumed to be hinged to the shell at its apex by a spring loaded double gimbal joint. Thus, the dumbbell has two degrees of freedom with respect to the shell. Damping is assumed at the hinges of the gimbal. The two tip masses of the dumbbell are assumed to be connected by a rigid link of negligible mass.

The reaction torques on the shell due to the relative motion between the dumbbell and the shell are given by,

$$C_x = \{k_z(\delta - \sigma_z) + c_z(\dot{\delta} - \dot{\sigma}_z)\} s\gamma \quad (4.46)$$

$$C_y = k_y(\gamma - \sigma_y) + c_y(\dot{\gamma} - \dot{\sigma}_y) \quad (4.47)$$

$$C_z = \{k_z(\delta - \sigma_z) + c_z(\dot{\delta} - \dot{\sigma}_z)\} c\gamma \quad (4.48)$$

where, k_y, k_z = torsional spring stiffness at the hinges of the gimbal

c_y, c_z = damping co-efficients at the hinges

γ, δ = dumbbell angle defined in Fig. 4.1b

σ_y, σ_z = small rotations of the shell at the gimbal due to elastic deformations.

The modal components of the reaction torques in Eqs. (4.46)-(4.48) can be expressed as,

$$\bar{E}_n = C_y \left. \frac{\partial \phi_x^{(n)}}{\partial z} \right|_{\substack{y=0 \\ z=0}} + C_z \left. \frac{\partial \phi_x^{(n)}}{\partial y} \right|_{\substack{y=0 \\ z=0}} \quad (4.49)$$

Eqs. (4.38)-(4.41) together with eqs. (4.46)-(4.49) describe the motion of the shallow shell. The equation of motion of the dumbbell in the $\tau_d(x_d y_d z_d)$ frame (see Appendix A) are given by,

$$\dot{\omega}_{y_d} - \omega_{x_d} \omega_{z_d} = G_{y_d} / I_d + \{k_y (\gamma - \sigma_y) + c_y (\dot{\gamma} - \dot{\sigma}_y)\} / I_d \quad (4.50)$$

$$\dot{\omega}_{z_d} + \omega_{y_d} \omega_{x_d} = G_{z_d} / I_d + \{k_z (\delta - \sigma_z) + c_z (\dot{\delta} - \dot{\sigma}_z)\} / I_d \quad (4.51)$$

where, $\omega_{x_d}, \omega_{y_d}, \omega_{z_d}$ = angular velocity components of the dumbbell.

G_{y_d}, G_{z_d} = gravity-gradient torques on the dumbbell.

In order to investigate the stability of the system about its nominal local horizontal orientation, Eqs. (4.38)-(4.41), (4.50) and (4.51) are linearized for small pitch (θ), roll (ϕ), yaw (ψ), γ , δ and elastic displacements. The linearized equations are presented in Eqs. (4.54)-(4.59). In deriving these equations we have used the results,

$$\sigma_y = \left. \frac{\partial q_x}{\partial z} \right|_{\substack{y=0 \\ z=0}} = \sum_n \epsilon_n C_z^{(n)} \quad (4.52)$$

$$\sigma_z = \left. \frac{\partial q_x}{\partial y} \right|_{\substack{y=0 \\ z=0}} = \sum_n \epsilon_n C_y^{(n)} \quad (4.53)$$

where, $\epsilon_n = A_n / \ell$; $C_y^{(n)} = \ell \left. \frac{\partial \phi_x}{\partial y} \right|_{\substack{y=0 \\ z=0}}$; $C_z^{(n)} = \ell \left. \frac{\partial \phi_x}{\partial z} \right|_{\substack{y=0 \\ z=0}}$

Since, $C_y^{(n)} = C_z^{(n)} = 0$ for all modes except for the modes with only one nodal diameter, it is evident from Eqs. (4.54)-(4.59) that in the linear range the pitch, roll, yaw, γ and δ motions are coupled to the elastic motion only through the axi-symmetric modes for which $I_1^{(n)} \neq 0$, and the modes with only one nodal diameter for which $C_y^{(n)} \neq 0$, $C_z^{(n)} \neq 0$.

$$\psi'' - \Omega_x \psi - (1 + \Omega_x) \phi' = 0 \quad (4.54)$$

$$\phi'' + 4\Omega_z \phi + (1 - \Omega_z) \psi' = \bar{c}_z \delta' + \bar{k}_z \delta - \sum_n (\bar{c}_n \epsilon_n' + \bar{k}_z \epsilon_n) C_y^{(n)} \quad (4.55)$$

$$0'' - 3\Omega_y \theta - 2 \sum_n \bar{c}_y \epsilon_n' I_1^{(n)} \frac{\ell}{J_y} = \bar{c}_y \gamma' + \bar{k}_y \gamma - \sum_n (\bar{c}_y \epsilon_n' + \bar{k}_y \epsilon_n) C_z^{(n)} \quad (4.56)$$

$$\begin{aligned} \epsilon_n'' + (\Omega_n^2 - 3) \epsilon_n + 2\theta' \frac{I_1^{(n)}}{M_n \ell} = & \frac{3I_1^{(n)}}{M_n \ell} + (\bar{c}_y \gamma' + \bar{k}_y \gamma) \frac{J_y}{M_n \ell^2} C_z^{(n)} \\ & + (\bar{c}_z \delta' + \bar{k}_z \delta) \frac{J_z}{M_n \ell^2} C_y^{(n)} - \sum_m (\bar{c}_y \epsilon_n' + \bar{k}_y \epsilon_n) C_z^{(mn)} \\ & - \sum_m (\bar{c}_z \epsilon_n' + \bar{k}_z \epsilon_n) C_y^{(mn)} \quad (n = 1, 2, \dots) \end{aligned} \quad (4.57)$$

$$\begin{aligned} \gamma'' + \bar{c}_y (1+c_1) \gamma' + \{3+\bar{k}_y (1+c_1)\} \gamma + 3(1+\Omega_y) \theta - (1+c_1) \sum_n (\bar{c}_y \epsilon_n' + \bar{k}_y \epsilon_n) C_z^{(n)} \\ + 2 \sum_n \bar{c}_y \epsilon_n' I_1^{(n)} \frac{\ell}{I_y} = 0 \end{aligned} \quad (4.58)$$

$$\begin{aligned} \delta'' + \bar{c}_z (1+c_2) \delta' + \{4+\bar{k}_z (1+c_2)\} \delta + 4(1-\Omega_z) \phi - (1-\Omega_z) \psi' \\ - (1+c_2) \sum_n (\bar{c}_z \epsilon_n' + \bar{k}_z \epsilon_n) C_y^{(n)} = 0 \end{aligned} \quad (4.59)$$

In the following sections the stability of the system when a finite number of elastic modes are retained in the model is considered.

The Case of a Rigid Shallow Spherical Shell

For rigid shallow shells, $\phi_x^{(n)} = 0$ for all n . This results in decoupling of Eqs. (4.54), (4.55) and (4.59) from Eqs. (4.56) and (4.58). Thus, the stability of the system for small initial conditions is governed by the following two independent characteristic equations.

$$\begin{vmatrix} s^2 - \Omega_x & -(1+\Omega_x)s & 0 \\ (1-\Omega_z)s & s^2 + 4\Omega_z & -(\bar{c}_z s + \bar{k}_z) \\ -(1+\Omega_z)s & 4(1+\Omega_z) & A_{\delta\delta} \end{vmatrix} = 0 \quad (4.60)$$

$$\begin{vmatrix} s^2 - 3\Omega_y & -(\bar{c}_y s + \bar{k}_y) \\ 3(1+\Omega_y) & A_{\gamma\gamma} \end{vmatrix} = 0 \quad (4.61)$$

$$\text{where, } A_{\delta\delta} = s^2 + (1+c_2) (\bar{c}_z s + \bar{k}_z) + 4$$

$$A_{\gamma\gamma} = s^2 + (1+c_1) (\bar{c}_y s + \bar{k}_y) + 3$$

For a perfectly symmetrical spherical shell, $\Omega_x = 0$. This results in Eq. (4.60) having a double root at the origin and, thus, rendering the system unstable in roll and yaw. To prevent this instability, it may be desirable to introduce a slight asymmetry in the structure such that $0 < |\Omega_x| \ll 1$.

After formal expansion of the characteristic determinants in Eqs. (4.60) and (4.61), we arrive at Eqs. (4.62) and (4.63).

$$s^6 + \alpha_1 s^5 + \alpha_2 s^4 + \alpha_3 s^3 + \alpha_4 s^2 + \alpha_5 s + \alpha_6 = 0 \quad (4.62)$$

$$s^4 + \alpha_7 s^3 + \alpha_8 s^2 + \alpha_9 s + \alpha_{10} = 0 \quad (4.63)$$

where, $\alpha_1 = \bar{c}_z (1+c_2)$

$$\alpha_2 = 5 + \bar{k}_z (1+c_2) - \Omega_z (\Omega_x - 3)$$

$$\alpha_3 = \bar{c}_z \{c_2 (1+3\Omega_z - \Omega_z \Omega_x) + 4 - \Omega_x\}$$

$$\alpha_4 = \bar{k}_z \{c_z (1+3\Omega_z - \Omega_z \Omega_x) + 4 - \Omega_x\}$$

$$+ 4\{1+3\Omega_z - 2\Omega_z \Omega_x\}$$

$$\alpha_5 = -4\bar{c}_z (c_2 \Omega_z + 1) \Omega_x$$

$$\alpha_6 = -\{\bar{k}_z (c_2 \Omega_z + 1) + 4\Omega_z\} 4\Omega_x$$

$$\alpha_7 = \bar{c}_y (1+c_1)$$

$$\alpha_8 = \bar{k}_y (1+c_1) + 3(1-\Omega_y)$$

$$\alpha_9 = 3\bar{c}_y (1-c_1 \Omega_y)$$

$$\alpha_{10} = 3\bar{k}_y (1-c_1 \Omega_y) - 9\Omega_y$$

$$-1 \leq \Omega_z < 0 \text{ and } 0 < \Omega_y \leq 1$$

After applying the Routh-Hurwitz criterion for stability, we arrive at the following necessary and sufficient conditions for the stability:

$$\bar{c}_z > 0$$

$$\bar{k}_z > \{\Omega_z (\Omega_x - 3) - 5\} / (1+c_2)$$

$$c_2 < (4 - \Omega_x) / (\Omega_z \Omega_x - 3\Omega_z - 1)$$

$$k_z > -4\{1+3\Omega_z - 2\Omega_z \Omega_x\} / \{c_2 (1+3\Omega_z - \Omega_z \Omega_x) + 4 - \Omega_x\}$$

$$\Omega_x < 0; \quad \bar{k}_z > \frac{-4\Omega_z}{1+c_2\Omega_z}$$

$$\bar{c}_y > 0; \quad \bar{k}_y > -3(1-\Omega_y)/(1+c_1)$$

$$c_1 < 1/\Omega_y; \quad \bar{k}_y > 3\Omega_y/(1-c_1\Omega_y)$$

and $\Delta_i > 0$ ($i = 1, \dots, 5$)

where, Δ_i 's are the principal minors of the determinant

$$\begin{vmatrix} \alpha_1 & 1 & 0 & 0 & 0 \\ \alpha_3 & \alpha_2 & \alpha_1 & 1 & 0 \\ \alpha_5 & \alpha_4 & \alpha_3 & \alpha_2 & \alpha_1 \\ 0 & \alpha_6 & \alpha_5 & \alpha_4 & \alpha_3 \\ 0 & 0 & 0 & \alpha_6 & \alpha_5 \end{vmatrix}$$

The condition $\Omega_x < 0$ implies that $J_y > J_z$. This can be achieved by adding two small concentrated masses at the ends of the diameter along the z-axis.

As \bar{k}_y and \bar{k}_z become very large, the characteristic roots corresponding to the lower frequency modes are, to a very good approximation, given by the roots of the following algebraic equations

$$s^4 + \alpha_4 s^2 + \alpha_6 = 0 \quad (4.64)$$

$$s^2 + \alpha_{10} = 0 \quad (4.65)$$

where, $\alpha_4 = \{c_2(1+3\Omega_z - \Omega_z\Omega_x) + 4 - \Omega_x\}/(1+c_2)$

$$\alpha_6 = -4(c_2\Omega_z + 1)\Omega_x/(1+c_2)$$

$$\alpha_{10} = 3(1-c_1\Omega_y)/(1+c_1)$$

The roots of Eqs. (4.64) and (4.65) are given by,

$$s_{1,2} \approx \pm i\sqrt{\alpha_6/\alpha_4}$$

$$s_{3,4} \approx \pm i\sqrt{\alpha_4}$$

$$s_{5,6} = \pm i\sqrt{\alpha_{10}}$$

For the values of the parameters given in Fig. 4.2 i.e. $c_2 = 0.9$, $\Omega_x = -.0001$, $c_1 = 0.9$, $H/a = 0.1$ we have

$$s_{1,2} = \pm i 4.2640143 \times 10^{-3}$$

$$s_{3,4} = \pm i 1.076055$$

$$s_{5,6} = \pm i 0.4090303$$

Fig. 4.2 shows the locus of the roots corresponding to the lowest frequency mode in the roll-yaw degree of freedom. The spring stiffness k_z is varied along each of these curves. It can be seen from these curves that by placing heavier concentrated masses at the ends of the diameter the roll-yaw stability can be improved.

The Case of a Shallow Spherical Shell with a Finite Number of Elastic Modes in the Model.

The mode shapes of a shallow spherical shell are characterized by a nodal pattern consisting of p ($p = 1, 2, \dots$) nodal diameters and j ($j = 1, 2, \dots$) concentric nodal circles centered about the axis of symmetry. For a perfectly symmetrical shell the position of the nodal diameter is arbitrary which is indicated by the arbitrariness of β_0 in Eq. (B.4) in Appendix - B. However, the addition of two small concentrated masses on the z -axis to make the shell slightly asymmetrical for roll-yaw stability, permits only two possible orientations of the nodal diameter:

- a. nodal diameter aligned along the roll axis (z axis) i.e. $\beta_0 = 0$.
- b. nodal diameter aligned along the pitch axis (y axis) of the plate i.e. $\beta_0 = \pi/2$.

Hence, the uncontrolled dynamics of the shell for each of these possible orientations of the nodal diameter is presented separately in the following sections.

A. The case of the nodal diameter along the pitch axis (y axis). For this position of the nodal diameter, $\beta_0 = \pi/2$, in Eq. (B.4) in Appendix B. Hence,

$$c_y^{(n)} = 0 \quad \text{for all } n$$

$$\text{and } c_z^{(n)} = \begin{cases} A_{j,1} \lambda_{j,1} (1+C_{j,1})/2, & p=1 \\ 0, & p \neq 1 \end{cases} \quad (4.66)$$

Hence, the roll (ϕ), yaw (ψ) and δ motions completely decouple from pitch, γ and elastic motions, i.e. (ψ, ϕ, δ) and $(\theta, \gamma, \epsilon_1, \dots, \epsilon_n)$ are two independent sets. Further, we consider only axis-symmetric modes and modes with only one nodal diameter in the present analysis. The other elastic modes are all independent in the uncontrolled dynamics.

The characteristic equation corresponding to the set (ψ, ϕ, δ) is given by Eq. (4.60). Thus, the shell behaves like a rigid body in the ψ, ϕ, δ degrees of freedom. The characteristic equation corresponding to the set $(\theta, \gamma, \varepsilon_1, \dots, \varepsilon_n)$ is given by,

$$\begin{vmatrix} s^2 - 3\Omega_y & -(\bar{c}_y s + \bar{k}_y) & (\bar{c}_y s + \bar{k}_y) C_z^{(1)} - 2I_1^{(1)} (\ell/J_y) \dots \\ 3(1 + \Omega_y) & A_{\gamma\gamma} & -(1 + c_1) (\bar{c}_y s + \bar{k}_y) C_z^{(1)} + 2I_1^{(1)} (\ell/J_y) \dots \\ 2I_1^{(1)} s / M_1 \ell & -(\bar{c}_y s + \bar{k}_y) \frac{J_y}{M_1 \ell^2} C_z^{(1)} & \vdots \\ \vdots & \vdots & \vdots \\ 2I_1^{(n)} s / M_n \ell & -(\bar{c}_y s + \bar{k}_y) \frac{J_y}{M_n \ell^2} C_z^{(n)} & A_{n,1} \dots \end{vmatrix} = 0 \quad (4.67)$$

where,

$$A_{\gamma\gamma} = s^2 + (1 + c_1)(\bar{c}_y s + \bar{k}_y) + 3$$

$$A_{mn} = (\bar{c}_y s + \bar{k}_y) C_z^{(mn)} \quad (m \neq n)$$

$$A_{nn} = s^2 + (\Omega_n^2 - 3) + (\bar{c}_y s + \bar{k}_y) \bar{C}_z^{(nn)}$$

If only one elastic mode is retained in the model Eq. (4.67) reduces to,

$$\begin{vmatrix} s^2 - 3\Omega_y & -(\bar{c}_y s + \bar{k}_y) & (\bar{c}_y s + \bar{k}_y) C_z^{(1)} - 2I_1^{(1)} (\ell/J_y) \\ 3(1 + \Omega_y) & A_{\gamma\gamma} & -(1 + c_1) (\bar{c}_y s + \bar{k}_y) C_z^{(1)} + 2I_1^{(1)} \frac{\ell}{J_y} \\ \frac{2I_1^{(n)}}{M_1 \ell} s & -(\bar{c}_y s + \bar{k}_y) \frac{J_y}{M_1 \ell^2} C_z^{(1)} & A_{1,1} \end{vmatrix} = 0$$

where, $A_{\gamma\gamma}$ and $A_{1,1}$ are defined in Eq. (4.67)

If the retained mode is an axis-symmetric mode, i.e., $C_z^{(1)} = 0$, Eq. (4.68) can be simplified to,

$$s^6 + \alpha_1 s^5 + \alpha_2 s^4 + \alpha_3 s^3 + \alpha_4 s^2 + \alpha_5 s + \alpha_6 = 0 \quad (4.69)$$

where, $\alpha_1 = (1 + c_1) \bar{c}_y$

$$\alpha_2 = (1 + c_1) \bar{k}_y + \Omega_1^2 - 3\Omega_y$$

$$\alpha_3 = \bar{c}_y \{ (1 + c_1)(\Omega_1^2 - 3) - 3c_1(1 + \Omega_y) \} + 4I_1^{(1)2} / M_1 J_y$$

$$\alpha_4 = \bar{k}_y \{ 3(1 - c_1 \Omega_y) + (1 + c_1)(\Omega_1^2 - 3) \} + 3\Omega_1^2(1 - \Omega_y) - 9 + \frac{4I_1^{(1)2}}{M_1 J_y} c_1 \bar{c}_y$$

$$\alpha_5 = 3(\Omega_1^2 - 3)(1 - c_1 \Omega_y) \bar{c}_y + \frac{4I_1^{(1)2}}{M_1 J_y} (c_1 \bar{k}_y + 3)$$

$$\alpha_6 = 3(\Omega_1^2 - 3)(1 - c_1 \Omega_y) \bar{k}_y - 9\Omega_y (\Omega_1^2 - 3)$$

The necessary conditions for stability are given by,

$$\bar{c}_y > 0 ; \quad \bar{k}_y > \frac{3\Omega_y - \Omega_1^2}{(1 + c_1)}$$

$$\Omega_1^2 - 3 > \left\{ 3c_1(1 + \Omega_y) - \frac{4I_1^{(1)2}}{M_1 I_y \bar{c}_y} \right\} / (1 + c_1)$$

$$\bar{k}_y > \left\{ 9 - 3\Omega_1^2(1 - \Omega_y) - \frac{4I_1^{(1)2} c_1 \bar{c}_y}{M_1 I_y} \right\} / \left\{ 3(1 - c_1 \Omega_y) + (1 + c_1)(\Omega_1^2 - 3) \right\}$$

$$\Omega_1^2 - 3 > - \frac{4I_1^{(1)2}}{M_1 I_y} (c_1 \bar{k}_y + 3) / 3(1 - c_1 \Omega_y) \bar{c}_y$$

$$\bar{k}_y > 3\Omega_y / (1 - c_1 \Omega_y) \tag{4.70}$$

If, on the otherhand, the retained mode is a mode with one nodal diameter for which, $I_1^{(1)} = 0$, Eq. (4.68) simplifies to,

$$s^6 + \alpha_1 s^5 + \alpha_2 s^4 + \alpha_3 s^3 + \alpha_4 s^2 + \alpha_5 s + \alpha_6 = 0 \tag{4.71}$$

where,

$$\alpha_1 / \bar{c}_y = 1 + c_1 + C^{(1,1)}$$

$$\alpha_2 = \bar{k}_y (\alpha_1 / \bar{c}_y) + \Omega_1^2 - 3\Omega_y$$

$$\alpha_3 / \bar{c}_y = (\Omega_1^2 - 3)(1 + c_1) - 3(1 - c_1 \Omega_y) + 3C^{(1,1)}(1 - \Omega_y)$$

$$\alpha_4 = \bar{k}_y (\alpha_3 / \bar{c}_y) + 3\Omega_1^2(1 - \Omega_y) - 9$$

$$\alpha_5 / \bar{c}_y = 3(\Omega_1^2 - 3)(1 - \Omega_y c_1) - 9\Omega_y C^{(1,1)}$$

$$\alpha_6 = \bar{k}_y (\alpha_5 / \bar{c}_y) - 9\Omega_y (\Omega_1^2 - 3)$$

The necessary conditions for stability are given by,

$$\bar{c}_y > 0$$

$$\bar{k}_y > - (\Omega_1^2 - 3\Omega_y) / (1 + c_1 + C^{(1,1)})$$

$$\begin{aligned}
\Omega_1^2 - 3 &> \{3(1 - c_1 \Omega_y) - 3C^{(1,1)}(1 - \Omega_y)\}(1 + c_1) \\
\bar{k}_y &> \{9 - 3\Omega_1^2(1 - \Omega_y)\} / (\alpha_3 / \bar{c}_y) \\
\Omega_1^2 - 3 &> 3\Omega_y C^{(1,1)} / (1 - \Omega_y c_1) \\
\bar{k}_y &> 9\Omega_y (\Omega_1^2 - 3) / (\alpha_5 / \bar{c}_y)
\end{aligned} \tag{4.72}$$

When more than one elastic mode is retained in the model, a formal expansion of the characteristic determinant in Eq. (4.67) is algebraically complicated. Hence, we employ a digital algorithm to evaluate the characteristic equation when all the system parameters are known. For this purpose Eqs. (4.56), (4.57) and (4.58) are re-written in the state variable form as,

$$\dot{\chi}' = \mathbf{A} \chi \tag{4.73}$$

where, $\chi = [\theta \ \gamma \ \varepsilon_1 \ \dots \ \varepsilon_n \ \theta' \ \gamma' \ \varepsilon'_1 \ \dots \ \varepsilon'_n]^T$

$$\mathbf{A} = \begin{bmatrix} 0 & | & \mathbf{I} \\ \hline \mathbf{P} & | & \mathbf{Q} \end{bmatrix}$$

0 = null matrix of size (n+2)x(n+2)

I = identity matrix of size (n+2)x(n+2)

$$\mathbf{P} = \begin{bmatrix} 3\Omega_y & \bar{k}_y & -\bar{k}_y C_z^{(1)} & \dots \\ -3(1 + \Omega_y) & -\{3 + \bar{k}_y(1 + c_1)\} & (1 + c_1)\bar{k}_y C_z^{(1)} & \dots \\ 0 & \bar{k}_y c_3 C_z^{(1)} & -(\Omega_1^2 - 3)\bar{k}_y C_z^{(1,1)} & \dots \\ \cdot & \cdot & \cdot & \dots \\ \cdot & \cdot & \cdot & \dots \\ \cdot & \cdot & \cdot & \dots \\ 0 & \bar{k}_y c_3 C_z^{(n)} & -\bar{k}_y C_z^{(n,1)} & \dots \end{bmatrix}$$

$$Q = \begin{bmatrix} 0 & \bar{c}_y & -\bar{c}_y C_z^{(1)} + 2I_1^{(1)} (\ell/J_y) & \dots \\ 0 & -(1+c_1)\bar{c}_y & (1+c_1)\bar{c}_y C_z^{(1)} - 2I_1^{(1)} (\ell/J_y) & \dots \\ -(2I_1^{(1)}/M_1 \ell) & \bar{c}_y c_3 C_z^{(1)} & -\bar{c}_y C_z^{(1,1)} & \dots \\ \vdots & \vdots & \vdots & \vdots \\ \vdots & \vdots & \vdots & \vdots \\ -(2I_1^{(n)}/M_n \ell) & \bar{c}_y c_3 C_z^{(n)} & -\bar{c}_y C_z^{(n,1)} & \dots \end{bmatrix} \quad (n+2) \times (n+2)$$

$$c_3 = J_y / M_n \ell^2$$

One can easily find the characteristic roots of the system of Eqs. (4.73) using a digital computer^{4,5}. The result of such an analysis is presented in Fig. 4.3. This figure shows the root loci of the lowest frequency mode of the system. It can be noted from the figure that the influence of the axi-symmetric modes, e.g. (1,0), (2,0) etc., on the other system modes is very weak. Since, the coupling between the axi-symmetric modes and the rigid body modes is very weak a negligible amount of damping is imparted into the axi-symmetric elastic modes. Hence, the characteristic roots corresponding to the axi-symmetric nodes lie very close to the imaginary axis. We also note from Fig. 4.3 that with an increase in spring stiffness, k, the characteristic roots corresponding to the lowest frequency modes move toward the imaginary axis.

B. The case of the nodal diameter along the roll axis (body z axis).

For this position of the nodal diameter, $\beta_0 = 0$ in Eq. (B.4) in Appendix -B. Hence,

$$c_z^{(n)} = 0$$

and

$$c_y^{(n)} = \begin{cases} A_{j,1} \lambda_{j,1} (1+C_{j,1})/2 & , p = 1 \\ 0 & , p \neq 1 \end{cases}$$

A study of Eqs. (4.54)-(4.59) reveals that for the present case, the roll (ϕ), yaw (ψ), δ motion and elastic modes with only one nodal diameter form an independent set from that of the pitch (θ), γ motion and the axi-symmetric elastic modes. Hence, we arrive at the following two independent characteristic equations for the system.

Roll-yaw $-\delta$

$$\begin{vmatrix}
 s^2 - \Omega_x & -(1 + \Omega_x)s & 0 & 0 & \dots \\
 (1 - \Omega_z)s & s^2 - 4\Omega_z & -(\bar{c}_z s + \bar{k}_z) & (\bar{c}_z s + \bar{k}_z) C_y^{(1)} & \dots \\
 -(1 - \Omega_z) & 4(1 - \Omega_z) & A_{\delta\delta} & -(1 + c_2)(\bar{c}_z s + \bar{k}_z) C_y^{(1)} & \dots \\
 0 & 0 & -(\bar{c}_z s + \bar{k}_z) c_3 C_y^{(1)} & A_{1,1} & \dots \\
 \cdot & \cdot & \cdot & \cdot & \dots \\
 \cdot & \cdot & \cdot & \cdot & \dots \\
 \cdot & \cdot & \cdot & \cdot & \dots \\
 0 & 0 & -(\bar{c}_z s + \bar{k}_z) c_3 C_y^{(n)} & A_{n,1} & \dots
 \end{vmatrix} = 0 \tag{4.75}$$

Pitch - γ - axi-symmetric modes

$$\begin{vmatrix}
 s^2 - 3\Omega_y & -(\bar{c}_y s + \bar{k}_y) & -2(I_1^{(1)} \ell / J_y) s & \dots \\
 3(1 + \Omega_y) & A_{\gamma\gamma} & 2(I_1^{(1)} \ell / J_y) s & \dots \\
 2(I_1^{(1)} / M_1 \ell) s & 0 & s^2 + \Omega_1^2 - 3 & 0 \dots 0 \\
 \cdot & \cdot & \cdot & \dots \\
 \cdot & \cdot & \cdot & \dots \\
 \cdot & \cdot & \cdot & \dots \\
 2(I_1^{(n)} / M_n \ell) s & 0 & 0 & 0 \dots s^2 + \Omega_n^2 - 3
 \end{vmatrix} = 0 \tag{4.76}$$

where,

$$\begin{aligned}
 A_{\delta\delta} &= s^2 + (1 + c_2)(\bar{c}_z s + \bar{k}_z) + 4 \\
 A_{mn} &= (\bar{c}_z s + \bar{k}_z) C_y^{(mn)} \quad (m \neq n) \\
 A_{nn} &= s^2 + \Omega_n^2 - 3 + (\bar{c}_z s + \bar{k}_z) C_y^{(nn)} \\
 A_{\gamma\gamma} &= s^2 + (1 + c_1)(\bar{c}_y s + \bar{k}_y) + 3 \\
 c_3 &= \frac{J_y}{M_n \ell^2}
 \end{aligned}$$

Since a formal expansion of the characteristic determinants in Eqs. (4.75) and (4.76) is involved, the numerical algorithm used in the previous cases is used to evaluate the characteristic equation and the characteristic roots. For this purpose we re-write Eqs. (4.54)-(4.59) in the following state variable form:

$$\dot{X}_1' = A_1 X_1 \quad (4.77)$$

$$\dot{X}_2' = A_2 X_2 \quad (4.78)$$

where, $X_1 = [\theta \ \gamma \ \varepsilon_{0,1} \ \varepsilon_{0,2} \ \dots \ \varepsilon_{0,n} \ \theta' \ \gamma' \ \varepsilon'_{0,1} \ \dots \ \varepsilon'_{0,n}]^T$
 $X_2 = [\psi \ \phi \ \delta \ \varepsilon_{1,1} \ \varepsilon_{1,2} \ \dots \ \varepsilon_{1,n} \ \psi' \ \phi' \ \delta' \ \varepsilon'_{1,1} \ \dots \ \varepsilon'_{1,n}]^T$
 $\varepsilon_{0,n}$ = non-dimensional modal amplitude of the nth axi-symmetric mode.
 $\varepsilon_{1,n}$ = non-dimensional amplitude of modes with one nodal diameter.

The characteristic roots of the system of Eqs. (4.77) and (4.78) can be found by using digital computer algorithm^{4,5}. The root loci of the lowest frequency mode of the system for the roll-yaw degree of freedom is presented in Fig. 4.4. It can be observed that this plot is very similar to the plot presented in Fig. 6 of Chapter 3. Thus, we see that the behavior of a free shallow spherical shell is very close to that of a flat circular plate. It is also observed that in the pitch degree of freedom, the axi-symmetric modes have negligible influence on the system characteristic roots corresponding to the lowest frequency modes.

REFERENCES

1. Reissner, E., "On Transverse Vibrations of Thin, Shallow Elastic Shells," Quart. Appl. Math, Vol. 13, No. 2, July 1955, pp. 169-176.
2. Johnson, M.W., Reissner, E., "On Transverse Vibrations of Shallow Spherical Shells", Quart. Appl. Math., Vol. 15, No.4, Jan. 1958, pp. 367-380.
3. Bainum, P.M., Kumar, V.K., James, P.K., "Dynamics and Control of Large Flexible Space Structures - Part B", NASA CR-156976 Report, May 1978.
4. Zadeh, L.A., Desoer, C.A., Linear System Theory, McGraw Hill Book Co., 1963.
5. Melsa, J.L., Jones, S.K., Computer Programs for Computational Assistance in the Study of Linear Control Theory, McGraw Hill Book Co., 1970.

$$J_x = \frac{1}{6} M(3a^2 + H^2)$$

$$J_y = J_z = M(1.5a^2 + H^2)/6$$

$$M = \pi \rho (a^2 + H^2)$$

$$dA = R^2 \sin \beta_1 d\beta_1 d\beta$$

$$r_c = R \sin \beta_1$$

$$\vec{r}_0 = \vec{r}_1 + \vec{r}_2$$

$$\vec{r}_2 = r_c \hat{e}_r + x_c \hat{i}$$

$$\vec{\omega} = \omega_x \hat{i} + \omega_y \hat{j} + \omega_z \hat{k}$$

$$= \omega_r \hat{e}_r + \omega_\beta \hat{\beta} + \omega_x \hat{i}$$

$$\frac{H}{a} \ll 1$$

$$(x+R-H)^2 + y^2 + z^2 = R^2$$

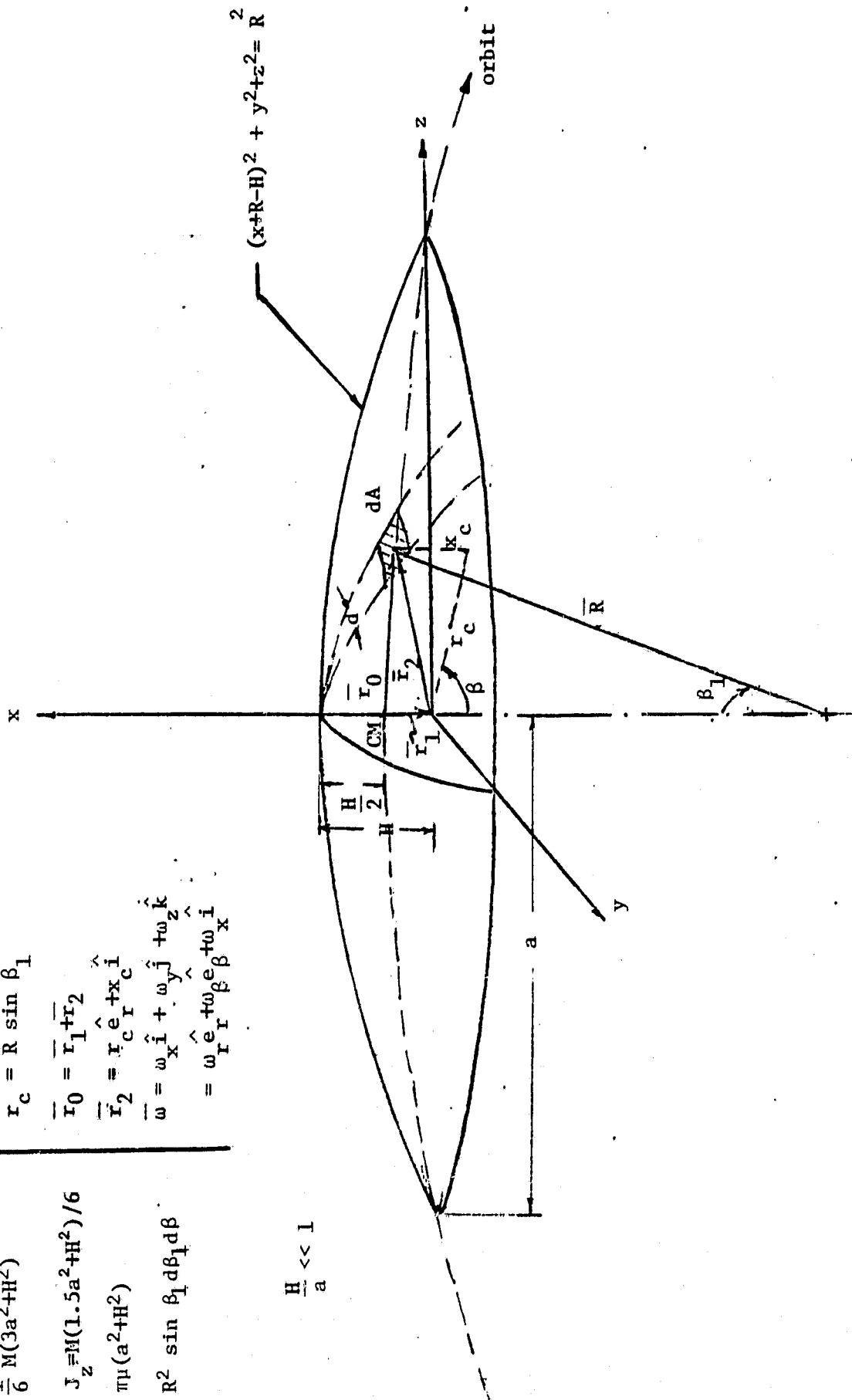
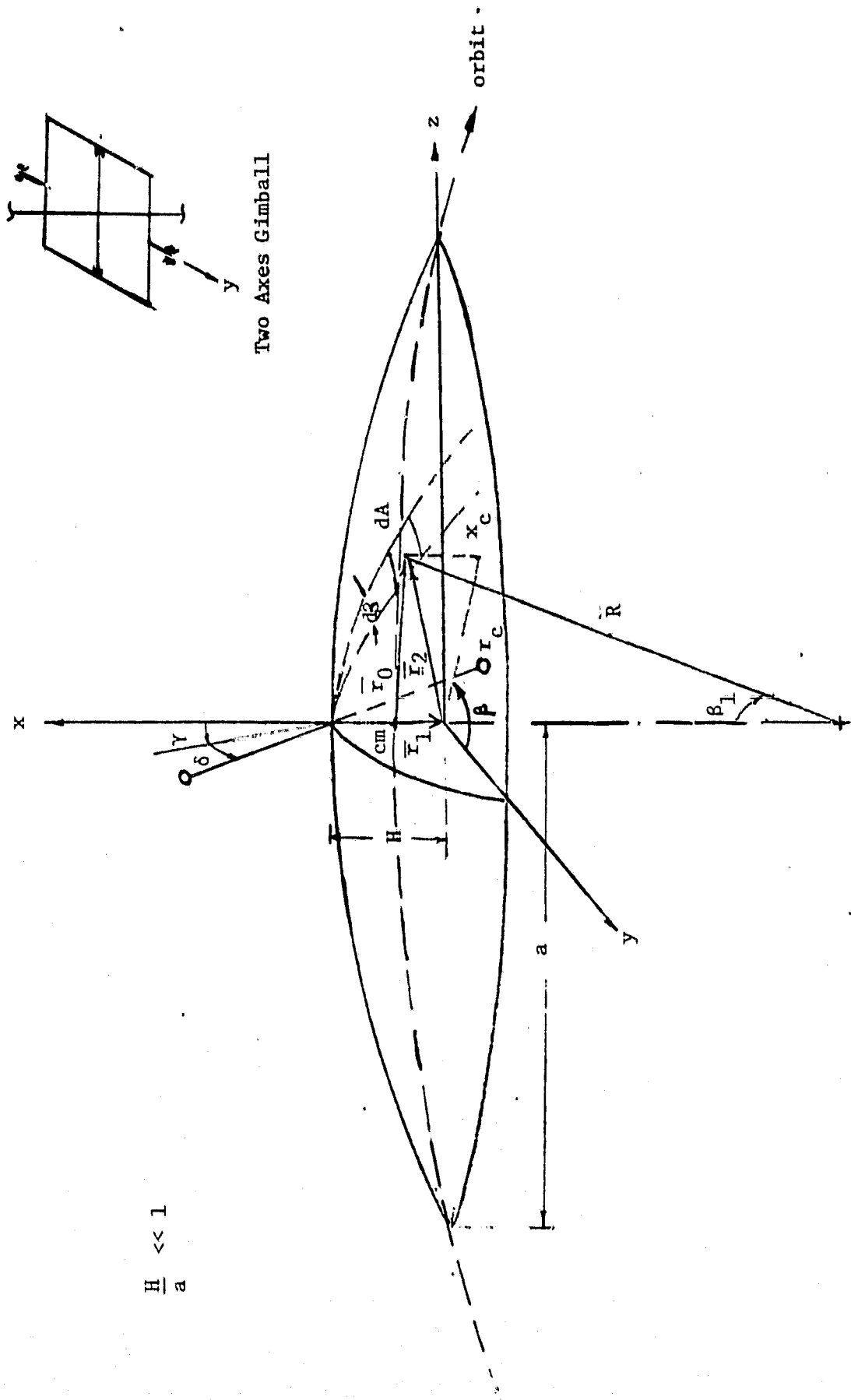


Fig 4.1a : Shallow Spherical Shell



$$\frac{H}{a} \ll 1$$

Two Axes Gimball

Fig. 4.lb: Shallow Spherical Shell with dumbbell

Roll-yaw degree of freedom

Damping ratio, $\zeta = 0.1$

Inertia ratio, $c_1 = 0.9$

$H/a = 0.1$

$$\Omega_x = \frac{J_y J_z}{J_x}$$

$$\Omega_x = -0.1$$

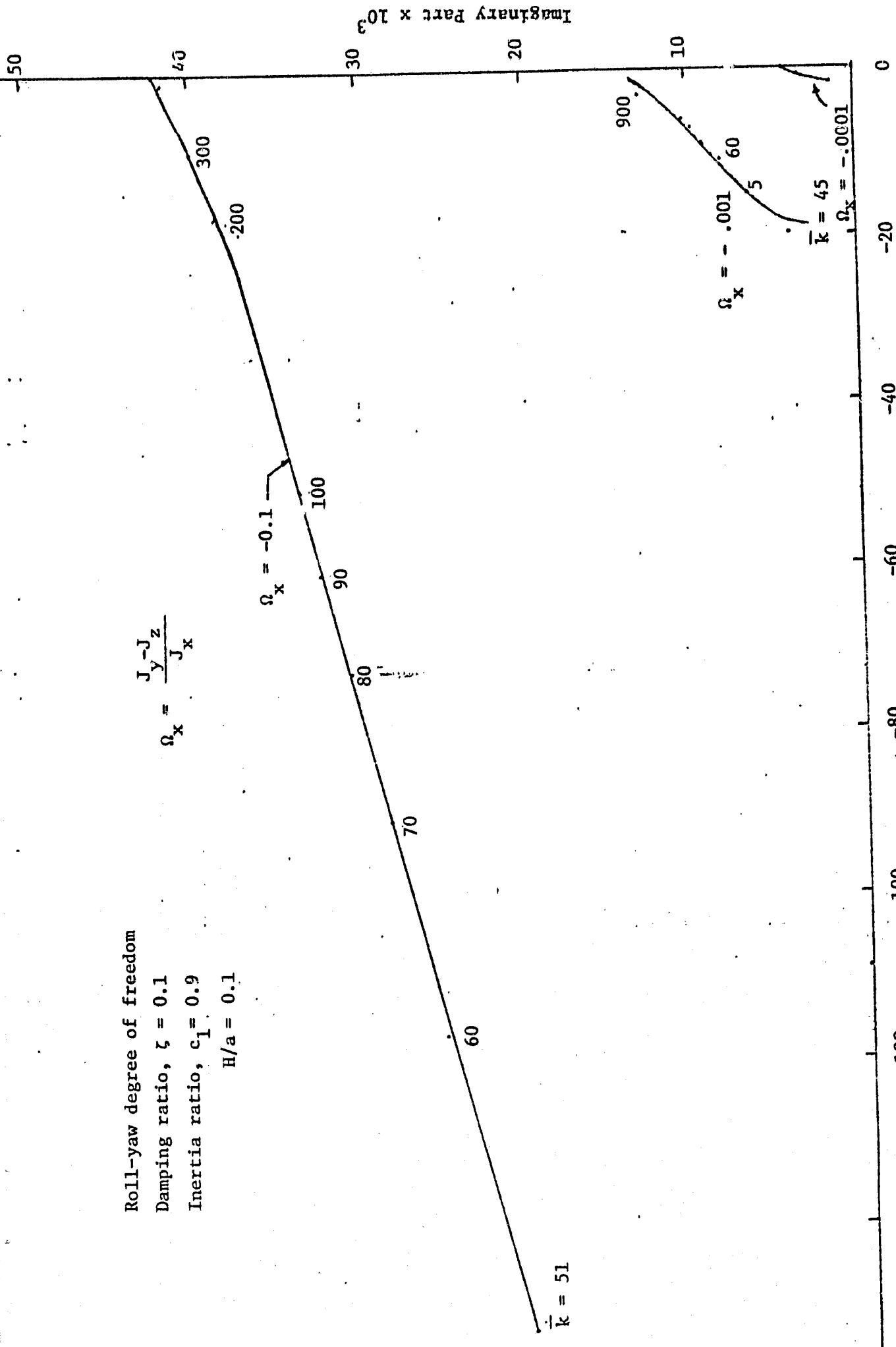


Fig. 4.2: Root Locus of Least Damped Mode - Rigid Shallow Spherical Shell with Dumbbell

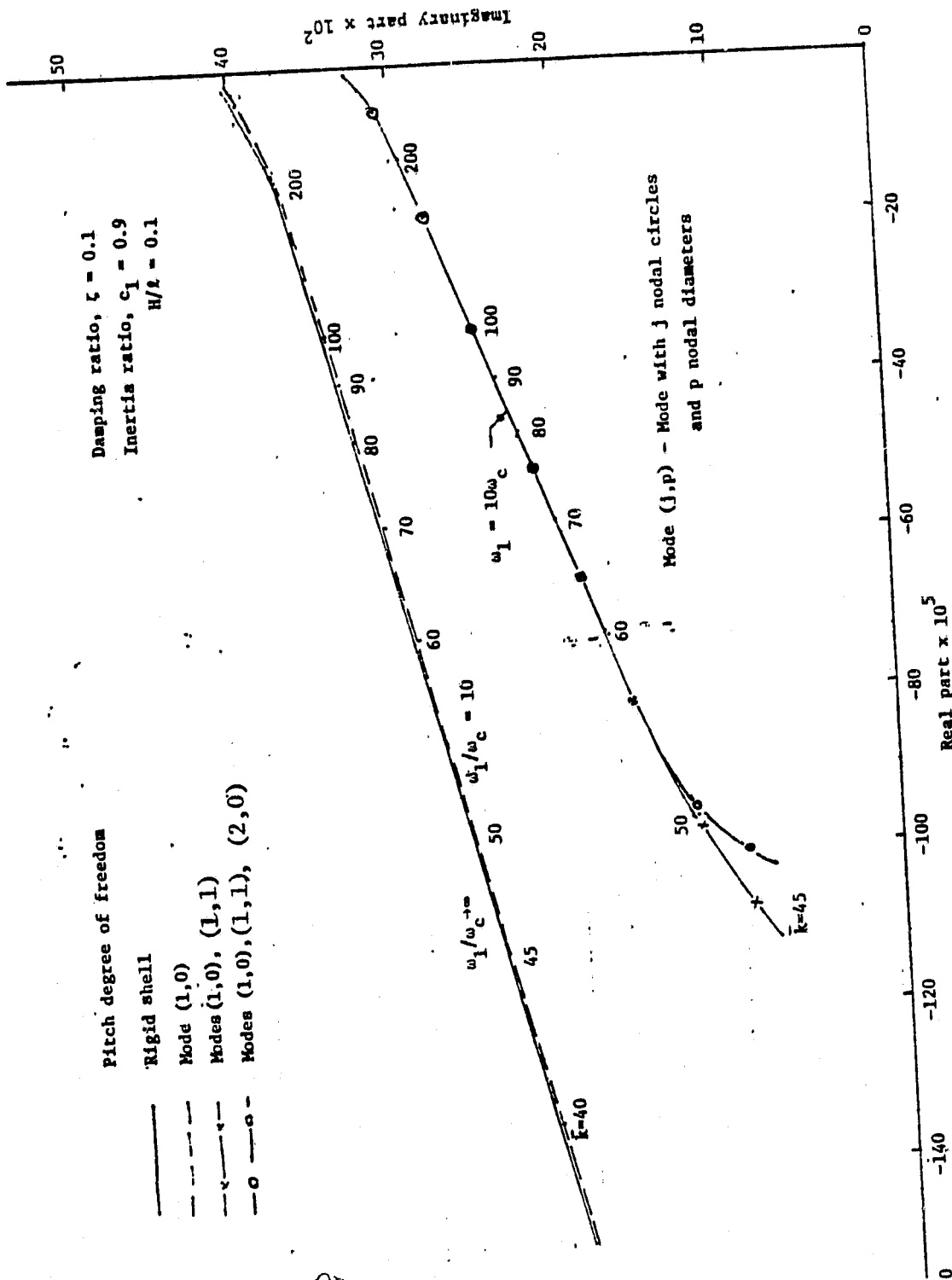


Fig. 4.3: Root Locus of Least Damped Mode - Shallow Sph. Shell with Dumbbell (Nodal Diameter Along Pitch Axis)

ORIGINAL PAGE IS OF POOR QUALITY

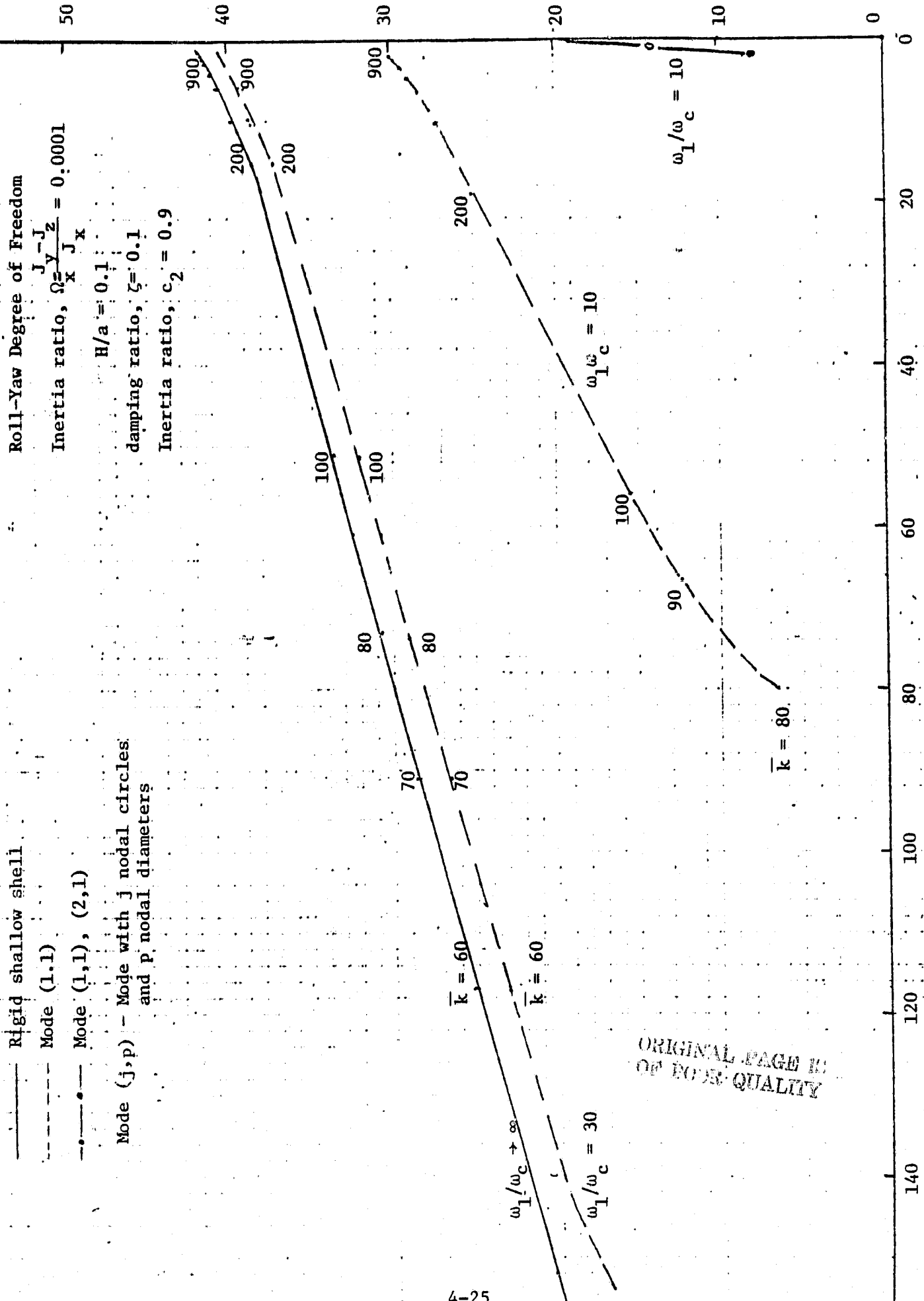


Fig. 4.4: Root Locus of Lowest Frequency Mode - Shallow Spherical Shell with Dumbbell

5A. CONCLUSIONS

1. Space structures with their maximum moment of inertia axis along the local vertical are gravitationally unstable. Such structures can be gravitationally stabilized by attaching a light weight dumbbell with heavy tip masses.
2. In the case of the flexible beam, the dumbbell excites only the anti-symmetric elastic modes of the beam.
3. In the case of the flat circular plate, the stabilizing dumbbell excites only those elastic modes with one nodal diameter. The small concentrated masses added for the roll-yaw stabilization of the plate result in only two possible positions for the nodal diameters.
4. In the case of the shallow spherical shell, the axi-symmetric modes are coupled to the pitch motion. In addition, the stabilizing dumbbell excites those elastic modes with one nodal diameter. The small concentrated masses added to stabilize roll-yaw result in only two possible positions for the nodal diameter.
5. The shallow shell undergoes a small static deformation under the action of gravity and centrifugal forces.
6. In all the cases above, as the torsional spring stiffness is increased, the characteristic roots of the least damped mode move toward the imaginary axis. The stability of the truncated model deteriorates with the increase in the number of elastic modes retained in the model.
7. To damp the motion of the system in all its modes, especially the low frequency modes, the use of active dampers (control systems) are needed. Moreover, it is thought that with the use of the passive gimballed dumbbell stabilization device together with active controllers, both the peak forces as well as fuel consumption could be significantly reduced. Such a study would represent a logical extension of the present work.

5B. RECOMMENDATIONS

Possible future contributions to this work could consist of: a study of the effects of higher order gravity-gradient potential terms and of solar radiation pressure for very large structures.

In the case of shell structures it was shown that the gravity and orbital motion can excite elastic modes of the structure. Hence, it is suggested to investigate the influence of orbital eccentricity on the elastic motion and find possible sources of resonance.

At the operational altitudes of the future missions involving large structures, the principal environmental disturbance is that due to solar radiation. Hence, it is proposed to develop accurate models for solar radiation pressure. Thermal gradients are also induced due to solar radiation which can excite some of the lower elastic modes of the structure. An investigation of the possible thermally induced structural oscillations is recommended.

APPENDIX - A

Kinematic Relations¹:

Fig (A.1) shows the sequence of Euler angle rotations adopted in going from orbit frame, $\tau_o(X_o, Y_o, Z_o)$ to the body frame, $\tau_b(X, Y, Z)$.

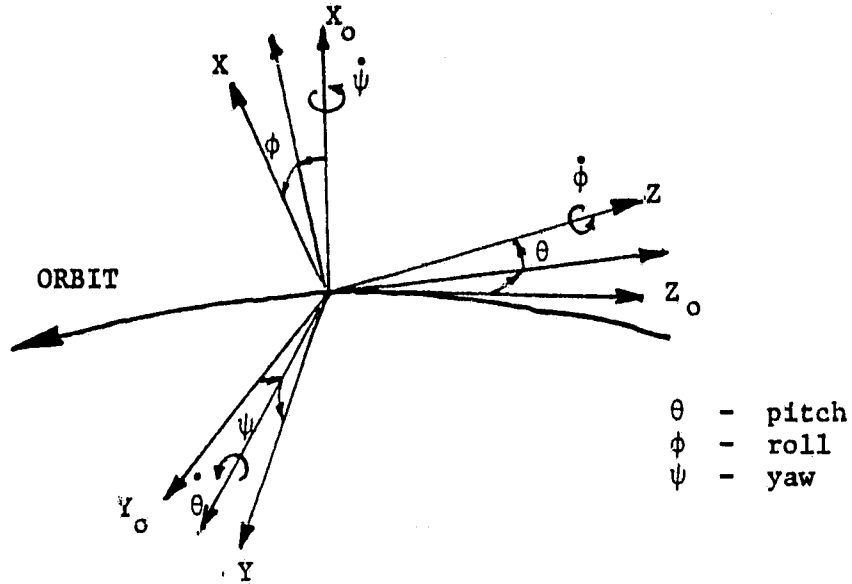


Fig. A.1: Euler angle rotations

The body frame, $\tau_b(X, Y, Z)$ and the orbit frame, $\tau_o(X_o, Y_o, Z_o)$ are related to each other by the following transformation relation,

$$\tau_b = T \tau_o \quad (A.1)$$

where,

$$T_1 = \begin{bmatrix} c\phi c\theta & s\phi c\psi + c\phi s\theta s\psi & s\phi s\psi - c\phi s\theta c\psi \\ -s\phi c\theta & c\phi c\psi - s\phi s\theta s\psi & c\phi s\psi + s\phi s\theta c\psi \\ s\theta & -c\theta s\psi & c\theta c\psi \end{bmatrix}$$

The body angular velocity components $(\omega_x, \omega_y, \omega_z)$ and Euler angular rates $(\dot{\theta}, \dot{\phi}, \dot{\psi})$ are related as follows,

$$\begin{aligned} \omega_x &= \dot{\theta} s\phi + \dot{\psi} c\phi c\theta - \omega_c (s\phi c\psi + c\phi s\theta s\psi) \\ \omega_y &= \dot{\theta} c\phi - \dot{\psi} s\phi c\theta - \omega_c (c\phi c\psi - s\phi s\theta s\psi) \\ \omega_z &= \dot{\psi} s\theta + \dot{\phi} + \omega_c c\theta s\psi \end{aligned}$$

The transformation between the co-ordinate frame, τ_c and the local cylindrical co-ordinate frame is as shown below.

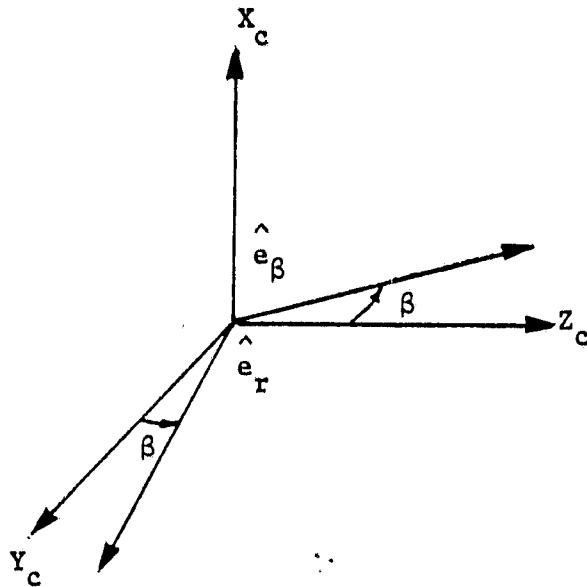


Fig. A.2

$$\begin{Bmatrix} A_x \\ A_y \\ A_z \end{Bmatrix}_{\tau_c} = T_4 \begin{Bmatrix} A_x \\ A_y \\ A_\beta \end{Bmatrix} \quad \text{local cylindrical frame}$$

where,

$$T_4 = \begin{bmatrix} 1 & 0 & 0 \\ 0 & c\beta & -s\beta \\ 0 & s\beta & c\beta \end{bmatrix}$$

(A.2)

Fig. (A.2) shows the sequence of γ and δ rotations adopted in arriving from body frame, τ_b , to the dumbbell frame, τ_d .

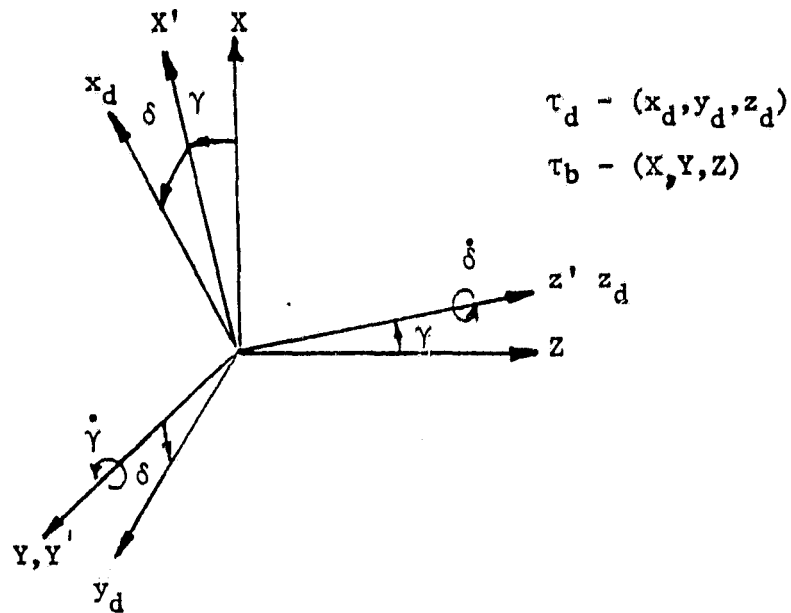


Fig. A.3

The body frame, τ_b , and the dumbbell frame, τ_d , are related to each other by the following transformation:

$$\tau_b = T_2 \tau_d$$

where,

$$T_2 = \begin{bmatrix} c\gamma c\delta & -c\gamma s\delta & s\gamma \\ s\delta & c\delta & 0 \\ -s\gamma c\delta & s\gamma s\delta & c\gamma \end{bmatrix} \quad (A.3)$$

APPENDIX B

Frequencies and Mode Shapes of a Shallow Spherical Shell*:

The results presented here are based on the following assumptions.

- the shell has constant thickness
- the vibration of the shell is primarily in the transverse direction i.e. parallel to shell's symmetry axis. The effect of longitudinal inertia is negligible in comparison with transverse inertia.

The natural frequencies of a thin, shallow spherical shell with completely free edge can be obtained from the roots ($\lambda_{1,p}, \lambda_{2,p}, \dots$) of the transcendental equations,

$$\frac{\lambda}{2} \left[\frac{J_p(\lambda)}{J_{p+1}(\lambda)} + \frac{I_p(\lambda)}{I_{p+1}(\lambda)} \right] = 1 - \nu \quad (p=0,1) \quad (B.1)$$

$$\omega_n > \omega_\infty : \quad \frac{\lambda^4}{\kappa^4} = \frac{S_p(\lambda)}{R_p(\lambda)} - 1 \quad (p=2,3,\dots) \quad (B.2)$$

$$\omega_n < \omega_\infty : \quad \frac{\eta^4}{\kappa^4} = \frac{U_p(\eta)}{V_p(\eta)} + 1 \quad (p=2,3,\dots) \quad (B.3)$$

where,

$$\lambda_{j,p}^2 = (\omega_n^2 - \omega_\infty^2)^{\frac{1}{2}} \ell^2 \sqrt{\frac{h\rho}{D}} \quad (j=1,2,\dots)$$

ω_n = natural frequency

ℓ = base radius of the shell

h = wall thickness of the shell

ρ = mass per unit volume of the material of the shell

D = flexural rigidity, $Eh^3/12(1-\nu^2)$

ν = Poisson's ratio

$$\omega_\infty = (C/h\rho R^2)^{\frac{1}{2}}$$

C = longitudinal stiffness factor, Eh

R = radius of curvature of the middle surface of the shell.

$J_p(\lambda), I_p(\lambda)$ = Bessel function and modified Bessel function of the first kind and order, p . Primes denote the derivative with respect to the argument.

$$S_p(\lambda) = 4^2 (p^2 - 1) (1 - \nu) \{ \lambda [J_p(\lambda) I_p'(\lambda) - J_p'(\lambda) I_p(\lambda)] \\ + (p+1) (1 - \nu) [I_p'(\lambda) - \frac{p}{\lambda} I_p(\lambda)] [J_p'(\lambda) - \frac{p}{\lambda} J_p(\lambda)] \}$$

*Extracted from Johnson, M.W. and Reissner, E., "On Transverse Vibrations of Shallow Spherical Shells," Quart. Appl. Math., Vol. 15, No. 4, Jan 1958, pp. 367-384.

$$R_p(\lambda) = \{(1-\nu) [\lambda J_p'(\lambda) - p^2 J_p(\lambda)] + \lambda^2 J_p(\lambda)\} \{(1-\nu) p^2 [\lambda I_p'(\lambda) - I_p(\lambda)] - \lambda^3 I_p'(\lambda)\} - \{(1-\nu) p^2 [\lambda J_p'(\lambda) - J_p(\lambda)] + \lambda^3 J_p'(\lambda)\} \times \{(1-\nu) [\lambda I_p'(\lambda) - p^2 I_p(\lambda)] - \lambda^2 I_p(\lambda)\}$$

$$\eta = \lambda i^{-3/2} \quad (i = \sqrt{-1}, \eta \geq 0)$$

$$U_p(\eta) = 2(1-\nu) p'(p^2-1) \{2^{3/2} p \eta (\text{ber}_p' \eta \text{bei}_p \eta - \text{ber}_p \eta \text{bei}_p' \eta) + 2^{1/2} (1-\nu) p(p+1) \left[\frac{p^2}{\eta^2} (\text{ber}_p^2 \eta + \text{bei}_p^2 \eta) - \frac{p}{\eta} (\text{ber}_p^2 \eta + \text{bei}_p^2 \eta)' + (\text{ber}_p' \eta)^2 + (\text{bei}_p' \eta)^2 \right]\}$$

$$V_p(\eta) = [(1-\nu^2) p^2 (p^2-1) - \eta^4] 2^{1/2} \eta (\text{ber}_p' \eta \text{bei}_p \eta - \text{ber}_p \eta \text{bei}_p' \eta) + 2^{1/2} (1-\nu) \eta^4 \{p^2 \left[\frac{1}{\eta} (\text{ber}_p^2 \eta + \text{bei}_p^2 \eta) \right]' - (\text{ber}_p' \eta)^2 - (\text{bei}_p' \eta)^2\}$$

$$\text{ber}_p \eta = \text{real part of } J_p(i^{3/2} \eta)$$

$$\text{bei}_p \eta = \text{imaginary part of } J_p(i^{3/2} \eta)$$

$$\kappa^4 = C \ell^4 / D R^2$$

The elastic mode shapes of the shallow spherical shell are given by the expression,

$$\phi^{(n)} = A_{j,p} \left[\frac{\lambda^{p+4}}{R D \lambda_{j,p}^4} C_{j,p} \zeta^{p+J_p(\lambda_{j,p} \zeta)} + D_{j,p} I_p(\lambda_{j,p} \zeta) \right] \cos p(\beta + \beta_0)$$

(B.4)

where,

p = Number of nodal diameters in the n^{th} mode

j = Number of nodal circles in the n^{th} mode

$\lambda_{j,p}$ = Roots obtained from eqns. (E.1), (B.2) and (B.3)

ζ = Non-dimensionalized radial distance, $0 \leq \zeta \leq 1$

β = angle defined in fig. B.1

β_0 = arbitrary phase angle

$C_{j,p}, D_{j,p}$ = constants determined from Eqns. (6.1)-(6.4) of Johnson and Reissner (1958)

$A_{j,p}$ = arbitrary constant

Thus, from Eq. (C.13) we can observe that the mode shapes of shallow spherical shells are characterized by a nodal pattern consisting of a set of concentric nodal circles (j) centered on symmetry axis and a set of nodal diameters (β). The modes with mode shapes having no nodal diameter ($\beta=0$) are called "axi-symmetric" modes. Thus, axi-symmetric mode shapes are dependent only on ζ .

The expressions for the constants $C_y^{(n)}, C_z^{(n)}$ are given by,

$$C_y^{(n)} = \frac{\partial \phi_x^{(n)}}{\partial \zeta} \Bigg|_{\substack{\zeta=0 \\ \beta=\pi/2}} = A_{j,1} \lambda_{j,1} [J_1'(0) + D_{j,1} I_1'(0)] \cos(-\frac{\pi}{2} + \beta_0) \quad (p=1)$$

$$= 0 \quad (p \neq 1)$$

Similarly,

$$C_z^{(n)} = \frac{\partial \phi_x^{(n)}}{\partial \zeta} \Bigg|_{\substack{\zeta=0 \\ \beta=0}} = A_{j,1} \lambda_{j,1} [J_1'(0) + D_{j,1} I_1'(0)] \cos \beta_0 \quad (p=1)$$

$$= 0 \quad (p \neq 1)$$

APPENDIX C

Evaluation of Integrals $I_{x_0}^{(j)}$, $I_{x_2}^{(j)}$ and $I_r^{(j)}$: From Eq. (B.13) of Appendix B we have,

$$W_{j,p}(\zeta) = A_{j,p} \left[\frac{\ell^{p+4}}{RD\lambda_{j,p}^4} C_{j,p} \zeta^{p+J_p}(\lambda_{j,p}\zeta) + D_{j,p} I_p(\lambda_{j,p}\zeta) \right] \quad (C.1)$$

Also, from the equation of a shallow spherical shell ($H \ll \ell$),

$$x_c(\zeta) = \frac{\ell^2}{2R} (1-\zeta^2) \quad (C.2)$$

By definition,

$$I_{x_0}^{(j)} = \int_0^1 x_c(\zeta) W_{j,0}(\zeta) \zeta d\zeta$$

i.e.

$$I_{x_0}^{(j)} = \frac{\ell^2}{2R} \int_0^1 \zeta(1-\zeta^2) [J_0(\lambda_{j,0}\zeta) + D_{j,0} I_0(\lambda_{j,0}\zeta)] d\zeta$$

Using the values of integrals given in Table - C1 and noting that $D_{j,0} = -J_1(\lambda_{j,0})/I_1(\lambda_{j,0})$ we obtain,

$$I_{x_0}^{(j)} = 2A_{j,0} \frac{\ell^2}{R} (1+\nu) J_1(\lambda_{j,0})/\lambda_{j,0}^3 \quad (C.3)$$

Now consider,

$$I_{x_2}^{(j)} = \int_0^1 x_c(\zeta) W_{j,2}(\zeta) \zeta d\zeta$$

i.e.

$$I_{x_2}^{(j)} = \frac{\ell^2}{2R} \int_0^1 \zeta(1-\zeta^2) \left[\frac{\ell^6}{RD\lambda_{j,2}^4} C_{j,2} \zeta^{2+J_2}(\lambda_{j,2}\zeta) + D_{j,2} I_2(\lambda_{j,2}\zeta) \right] d\zeta$$

Hence using the values of integrals listed in Table C1 we get,

$$I_{x_2}^{(j)} = \frac{\ell^2}{2R} A_{j,2} \left[\frac{\ell^6}{12RD\lambda_{j,2}^4} C_{j,2} + \frac{D_{j,2}}{\lambda_{j,2}^3} \{2\lambda_{j,2}(I_0(\lambda_{j,2})+1) - 8I_1(\lambda_{j,2})\} \right. \\ \left. + \frac{1}{\lambda_{j,2}^3} \{2\lambda_{j,2}(J_0(\lambda_{j,2})+1) - 8J_1(\lambda_{j,2})\} \right] \quad (C.4)$$

Similarly, consider

$$\begin{aligned}
 I_r^{(j)} &= \int_0^1 \zeta^2 W_{j,3}(\zeta) d\zeta \\
 &= \int_0^1 \zeta^2 \left[\frac{\ell^7}{RD\lambda_{j,3}^4} C_{j,3} \zeta^{3+J_3(\lambda_{j,3}\zeta)} + D_{j,3} I_3(\lambda_{j,3}\zeta) \right] d\zeta
 \end{aligned}$$

Using the values of the integrals given in Table C 1, we arrive at,

$$\begin{aligned}
 I_r^{(j)} &= \frac{\ell^7}{6RD\lambda_{j,3}^4} C_{j,3} + \frac{1}{\lambda_{j,3}^3} [(8-8J_0(\lambda_{j,3}) - 4\lambda_{j,3} J_1(\lambda_{j,3}) - \lambda_{j,3}^2 J_2(\lambda_{j,3})) \\
 &+ \frac{D_{j,3}}{\lambda_{j,3}^3} \{ \lambda_{j,3}^2 I_2(\lambda_{j,3}) - 4\lambda_{j,3} I_1(\lambda_{j,3}) + 8I_0(\lambda_{j,3}) - 8 \}] \quad (C.5)
 \end{aligned}$$

Table C1: Some Useful definite integrals.

$\int_0^1 \zeta J_0(\lambda \zeta) d\zeta$	$J_1(\lambda) / \lambda$
$\int_0^1 \zeta^3 J_0(\lambda \zeta) d\zeta$	$[\lambda^2 J_1(\lambda) + 2\lambda J_0(\lambda) - 4J_1(\lambda)] / \lambda^3$
$\int_0^1 \zeta J_2(\lambda \zeta) d\zeta$	$-[\lambda J_1(\lambda) + 2J_0(\lambda) - 2] / \lambda^2$
$\int_0^1 \zeta^3 J_2(\lambda \zeta) d\zeta$	$[8J_1(\lambda) - 4\lambda J_0(\lambda) - \lambda^2 J_1(\lambda)] / \lambda^3$
$\int_0^1 \zeta^2 J_3(\lambda \zeta) d\zeta$	$[8 - 8J_0(\lambda) - 4\lambda J_1(\lambda) - \lambda^2 J_2(\lambda)] / \lambda^3$
$\int_0^1 \zeta I_0(\lambda \zeta) d\zeta$	$I_1(\lambda) / \lambda$
$\int_0^1 \zeta^3 I_0(\lambda \zeta) d\zeta$	$[\lambda^2 I_1(\lambda) - 2\lambda I_0(\lambda) + 4I_1(\lambda)] / \lambda^3$
$\int_0^1 \zeta I_2(\lambda \zeta) d\zeta$	$[\lambda I_1(\lambda) - 2I_0(\lambda) + 2] / \lambda^2$
$\int_0^1 \zeta^3 I_2(\lambda \zeta) d\zeta$	$[\lambda^2 I_1(\lambda) - 4\lambda I_0(\lambda) + 8I_1(\lambda)] / \lambda^3$
$\int_0^1 \zeta^n d\zeta$	$\frac{1}{n+1}$
$\int_0^1 \zeta^2 I_3(\lambda \zeta) d\zeta$	$[\lambda^2 I_2(\lambda) - 4\lambda I_1(\lambda) + 8I_0(\lambda) - 8] / \lambda^3$